Compact Doppler Radar System for Heart Rate Detection

A THESIS SUBMITTED TO THE GRADUATE DIVISION OF THE UNIVERSITY OF HAWAI'I IN PARTIAL FULFILLMENT OF THE REQUIREMENTS FOR THE DEGREE OF

MASTER OF SCIENCE

IN

ELECTRICAL ENGINEERING

MAY 2007

By

Shuhei Yamada

Thesis Committee:

Victor M. Lubecke Chairperson

Olga Boric-Lubecke

Anders Host-Madsen

We certify that we have read this thesis and that, in our opinion, it is satisfactory in scope and quality as a thesis for the degree of master of science in Electrical Engineering.

THESIS COMMITTE

Chairperson

Acknowledgements

The author would like to thank Professor Victor M. Lubecke, Olga Boric-Lubecke, and Host-Madsen for very useful advices and discussions especially Professor Victor M. Lubecke for his great support as my supervisor. The author also would like to thank Byung-Kwon Park, Iun Lo, Wansuree Massagram, Xiaoyue Wang, Mingqi Chen, Noah Hafner, Yun Pyo Hong, Dung Phuong Nguyen, Alex Vergara, Issar Mostafanezhad, John E Kiriazi, Qin Zhou, and Nicolas Petrochilos for their great help.

Abstract

Periodic motion, such as that resulting from cardiopulmonary activity, can be measured with a microwave Doppler radar system. This thesis focuses on the assessment of radio system requirements and critical specifications for such radar sensing systems. The fundamental limitations for transmit power, receive power and range for a functional 2.4GHz IMS band cardiopulmonary radar system were computed and measured, including free space losses, noise, and fundamental heart rate detection limits. The minimum required power for close range rate detection was also assessed. Heart rates for subjects holding their breath or breathing normally were successfully tracked for signal power levels as low as 20 nW. This is the lowest power ever reported for an ISM band CW Doppler radar for heart rate detection. These results can be extrapolated to higher power systems where obstructions and antenna gain similarly impact the signal power available for heart motion detection. A 2.4GHz microwave Doppler radar system was designed for the required assessments, with several transceiver variations fully integrated on printed circuit boards using various antenna configurations. The transceiver boards were 101.6[mm] by 111.6[mm], and included a small on-board oscillator. A multiple antenna system was used to provide more comprehensive data for advanced signal processing, and the modular system could be easily expanded. Issues and means for performance improvement of the system are also reported. Sensitivity was found to be limited by direct conversion architecture and component issues. for which several circuit configurations were explored, acheiving significant DC offset and LO leakage reduction. Using DC offset cancelling, flicker noise reduction was also achieved, which significantly affects the SNR at baseband and improved the system sensitivity.

Table of Contents

List of Figures

List of Tables

CHAPTER1

INTRODUCTION

With the rapid development of radio applications such as cell phones, wireless LAN, and Bluetooth, the demands for and availability of new wireless technologies are increasing. Through the availability of increasing computational power, the hardware for these applications can be developed with low cost, small size, high performance, and multi-tasking capability. Those developments can be extended to biomedical engineering and medical practice through the production of high performance medical equipment, particularly for addressing outpatient and chronic healthcare demands fueled by an aging population. Requirements for this equipment are low cost, high performance, high accuracy, small size, and safety. One promising new technology which exploits developments in wireless and computational technologies is Doppler-radar for remote sensing of cardiopulmonary activity, which has great potential for health monitoring and personnel detection.

Doppler radar systems are well known for speed detection, such as the "radar gun" speed gauge which police officers use to detect the speed of cars. This speed gauge utilizes the characteristics of Doppler radar sensing. By applying the same Doppler radar sensing techniques for medical applications, the speed and displacement of human body movement such as that associated with heart beat and breathing can be detected. This technique eliminates the intrusive cables typically associated with conventional heart rate measurement equipment, thus providing easier and more accurate health monitoring. Doppler radar monitoring systems generally transmit a continuous wave signal while receiving and

demodulating the signal's reflection from a target. When the target has time-varying movement with zero net velocity, the reflected signal is phase-modulated in proportional to the position of the target rather than the velocity. A stationary human body presents two independent time varying movements with zero net velocity based on respiration and cardiac activity, and the largest reflection of incident RF power occurs at the body surface. Thus, the phase of a reflected signal will be proportional to positional variations across the body surface corresponding to motion of the heart and lungs. Applications of Microwave Doppler radar systems include medical equipment for patients who have a heart disease or sleep apnea syndrome, baby monitoring in order to avoid sudden unexpected death, disaster rescue where the system can detect cardiopulmonary signals from people trapped in debris, and military usage to detect people who hiding behind walls, or count the number of people hidden in a room.

The in addition to application specific signal processing detection and separation algorithms and associated high speed compact computational hardware, these systems are keenly dependent on the development of low-cost high-performance compact radio transceivers. The demands of such real-time, short range, high-precision Doppler radar applications are a new challenge, and the resulting requirments for radio architectures and hardware have not yet been established. In this thesis various quadrature direct conversion microwave Doppler radar systems have been developed to explore the requirements needed for practical cardiopulmonary monitoring. Several hybrid microwave tranceivers were fabricated and studied, with the intent of ultimately developing even more compact integrated circuit solutions that would meet requirements while allowing cost-effective mass

production. Issues such as signal power, isolation and noise were identified along with corresponding mitigation approaches.

This thesis consists of six chapters. In chapter 1, an introduction to microwave Doppler radar for human cardiopulmonary activity detection is presented. It includes background and applications, and illustrates the purpose, and goals of this research. In chapter 2, the basic theory of microwave Doppler radar systems is described to provide the basic and principles of radar sensing techniques needed to understand the contents of this thesis. This includes basic radar principles, the Doppler effect, and a derivation and explanation of radar range equations. In the chapter 3, considerations for using a Doppler radar system to assess the limitations and requirements for heart rate detection are described. In the chapter 4, the design of several Doppler radar systems is described, along with the measurement and analysis of fabricated Doppler radar systems. Based on the measurement results and considerations, the issues and means for performance improvement of such Doppler radar systems is described in chapter 5. Chapter 6, provides the conclusion.

CHAPTER 2

DOPPLER RADAR THORY

2.1 Radar Basics

Radar is an acronym for **Ra**dio **D**etection **a**nd **R**anging; thus it is used for detecting a target's presence and distance from the user. The basic principle of operation of radar is simple to understand. However, the theory behind it can be quite complex. An understanding of the theory is essentially in order to be able to specify and operate radar systems correctly. The implementation and operation of radar systems involves a wide range of disciplines such as building works, heavy mechanical and electrical engineering, high power microwave engineering, and advanced high speed signal and data processing techniques. Radar measurement of range, or distance, is made possible because of the properties of radiated electromagnetic energy. This energy normally travels through space in a straight line, at a constant speed, and will vary only slightly because of atmospheric and weather conditions. Electromagnetic energy travels through air at approximately the speed of light. The electromagnetic waves are reflected if they meet an electrically disruptive surface. If these reflected waves are registered again at the place of their origin, then that means an obstacle is in the propagation direction. The electronic principle on which radar operates is very similar to the principle of sound-wave reflection. If you shout in the direction of a sound-reflecting object, you will hear an echo. If you know the speed of sound in air, you can then estimate

the distance and general direction of the object. The time required for an echo to return can be roughly converted to distance if the speed of sound is known. Radar uses electromagnetic energy pulses in much the same way. The radio-frequency energy is transmitted to and reflected from the object. A small portion of the reflected energy returns to the radar set. This returned energy is called an ECHO, just as it is in sound terminology. Radar sets use the echo to determine the direction and distance of the reflecting object. The distance is determined from the running time of the transmitted signal and the propagation speed. The actual range of a target from the radar is known as slant range. Slant range is the line of sight distance between the radar and the object illuminated. While ground range is the horizontal distance between the emitter and its target and its calculation requires knowledge of the target's elevation. Since the waves travel to a target and back, the round trip time is divided by two in order to obtain the time the wave took to reach the target. Therefore the following formula arises for the slant range:

$$R = \frac{C \cdot t}{2} \qquad \text{(Eq. 2.1)}$$

Where C_0 = speed of light = $3 \cdot 10^8$ $^m/_s$, t = measured time [s], R = slant range [m]

The Distances are expressed in kilometers or nautical miles.

2.2 Classification of Radar Systems

There are several types of radar systems which are classified by the detection purpose, target, configuration, method, etc. In this section, the classification of radar systems is described, as illustrated in Fig. 2.1.

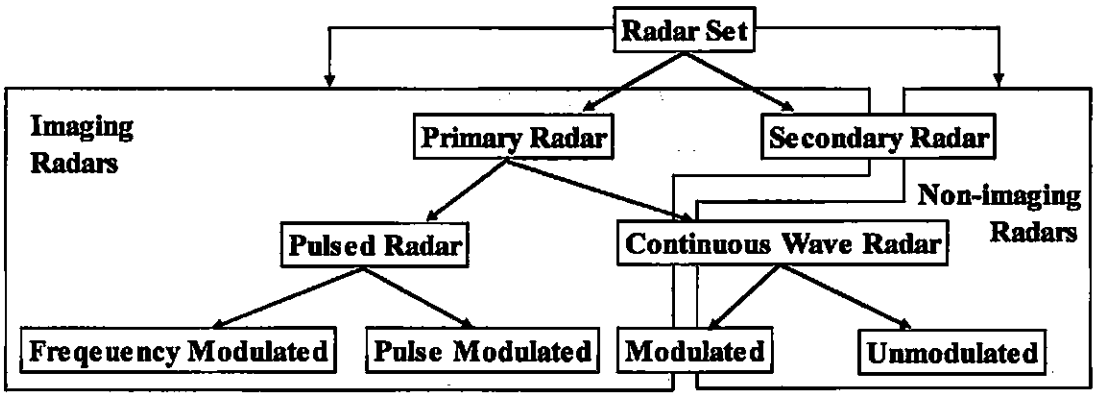

Fig 2.1. Classification of Radar Systems

2.2.1 Imaging Radar and Non-Imaging Radar

An Imaging Radar forms a picture of the observed object or area. Imaging radars have been used to map the Earth, other planets, asteroids, other celestial objects, and to categorize targets for military systems. Typical implementations of Non-Imaging Radar system are for speed gauges and radar altimeters. These are also called scatterometers since they measure the scattering properties of the object or region being observed. Non-Imaging Secondary Radar applications include immobilizer systems found in some recent commercial automobiles.

2.2.2 Primary Radar

A Primary Radar transmits high-frequency signals which reflect upon incidence with targets. The resulting echoes are received and evaluated. Unlike secondary radar sets, primary radar units receive their echoes of their own emitted signals.

2.2.3 Secondary Radar

For secondary radar, targets, like aircraft, must have a transponder (transmitting responder) on board, and this transponder responds to interrogation by transmitting a coded reply signal. This response can contain much more information, than a primary radar unit is able to acquire, like data on altitude, identification codes, or notification of technical problems on board the aircraft.

2.2.4 Pulsed Radars

Pulse radar sets transmit a high-frequency impulse signal of high power. After this impulse signal, a longer break follows in which the echoes can be received, before a new transmitted signal is sent out. Direction, distance, and sometimes if necessary the height or altitude of the target can be determined from the measured antenna position and propagation time of the pulse-signal.

2.2.5 Unmodulated CW- Radar

The transmitted signal of for CW radar is constant in amplitude and frequency. This equipment is specialized for speed measurment. Distances cannot be measured, e.g. they are used as speed gauges for police. Newer related techniques like LIDAR work similarly in the IR-laser frequency range.

2.2.6 Continuous Wave Radar

Continuous wave radar systems transmit a continuous wave radio signal to detect information for a target. In this type of radar system, a known frequency signal is transmitted and the reflected signal from the target is received. The main advantage of the CW radar systems is that they are not pulsed, and have no minimum or maximum range, and maximize the power incident on the target. CW radars have the disadvantage that they cannot measure distance, because there is no time reference in the continuous wave. In order to correct for this problem, frequency shifting methods can be used. When a reflection is received the frequencies can be examined, and by knowing when in the past that particular frequency was sent out, you can do a range calculation similar to using a pulse. It is generally not easy to make a transmitter that can send out random frequencies cleanly, so instead frequency-modulated CW radars (FMCW) use a smoothly varying ramp of frequencies, up and down.

2.3 Radar Cross Section

When an electromagnetic wave hits a target, it is scattered. For radar systems, one of the most important things the strength of the electromagnetic wave intensity which comes back opposite to the incident direction, and such a wave is called back scatter. In radar techniques, the radar cross section, σ, is used in order to quantify the intensity of back scatter. In Fig. 2.2, the radar cross section of a sphere is shown.

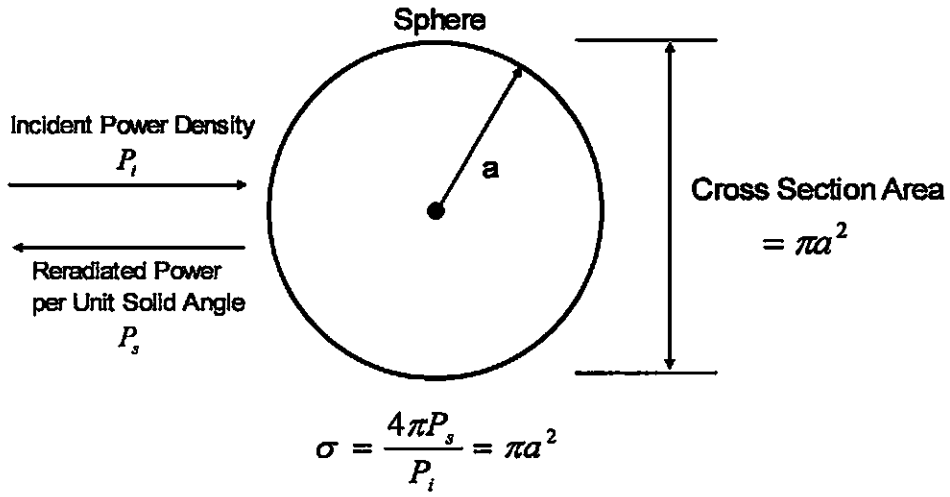

Fig. 2.2. Radar cross-section of a sphere

2.4 Doppler- Effect

The Doppler- Effect is the apparent change in frequency or pitch when a sound wave source moves either toward or away from the listener, or when the listener moves either toward or away from the sound source. This principle, discovered by the German physicist Christian Doppler, applies to all wave motion. The apparent change in frequency between the source of a wave and the receiver of the wave is due to relative motion between the source and the receiver. To understand the Doppler effect, first assume that the frequency of a sound from a source is held constant. The wavelength of the sound will also remain constant. If both the source and the receiver of the sound remain stationary, the receiver will hear the same frequency sound produced by the source. This is because the receiver is receiving the same number of waves per second that the source is producing. Now, if either the source or the receiver or both move toward the other, the receiver will perceive a higher frequency sound. This is because the receiver will receive a greater number of sound waves per second and interpret the greater number of waves as a higher frequency sound. Conversely, if the

source and the receiver are moving apart, the receiver will receive a smaller number of sound waves per second and will perceive a lower frequency sound. In both cases, the frequency of the sound produced by the source will have remained constant.

2.5 Doppler Radar

Doppler radar can detect the position and velocity of the target by measuring Doppler frequency shift. When a target is going away from the radar, the wavelength of the wave reflected by the target is increased by the Doppler effect. On other hand, when the target is coming closer to the radar, the wavelength of reflected wave is decreased by the Doppler effect. By measuring this wavelength change, the radar can detect how fast the target is moving with respect to the radar. However, if the target is moving perpendicularly to the radar, it does not make any Doppler shift. Therefore the radar can not distinguish movement and that case. A Doppler radar only can detect one dimensionally, so for detection in two dimensions, another Doppler radar is used at the same time. By analyzing the results of such a multiple radar system, two dimensional movement of a target is detectable. In Fig. 2.3, the basic theory of Doppler radar system is shown. A local oscillator signal LO represented by

$$T(t) = \cos(2\pi f_t t + \phi(t)) \qquad \text{(Eq. 2.2)}$$

Where f_t is the frequency of the transmitting signal, and $\phi(t)$ is the phase noise of oscillator. After the signal reflected by the target, the signal represented by

$$R(t) = \cos(2\pi f_t t + \theta + p(t) + \phi(t - \frac{2R}{c})) \qquad \text{(Eq. 2.3)}$$

Where θ is the constant phase shift, and $p(t)$ is the phase signal by the movement of the target. After mixed the LO signal and received signal, the movement information of target can be expressed as

$$B(t) = \cos(\theta + p(t) + \Delta\phi(t)) \qquad \text{(Eq. 2.4)}$$

Where $\Delta\phi(t)$ is the residual phase noise.

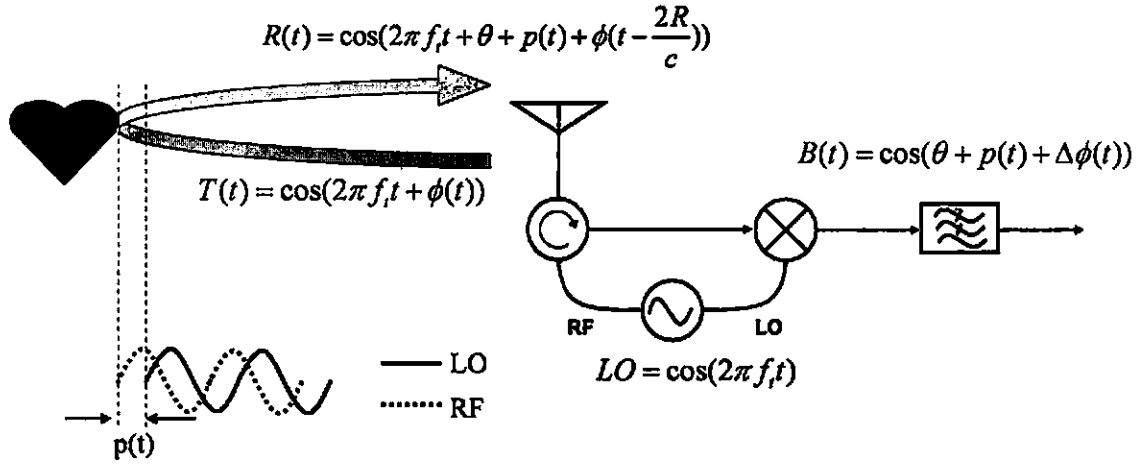

Fig. 2.3. The basic principle of Doppler radar

2.6 Radar Range Equation

Range is the distance from the radar site to the target measured along the line of sight. If the respective running time, t, is known, then the distance, R, between a target and the radar set can be calculated by using the "Radar range equation". The radar equation represents the physical dependence on propagation through space for the systems transmitted power. Furthermore, one can assess the performance of the radar with the radar equation.

Assuming that electromagnetic waves propagate under ideal conditions, i.e. without dispersion. If high-frequency energy is emitted by an isotropic antenna, then the energy is

propagated uniformly in all directions. The energy density spreads spherically. Therefore at the point distant R from the radar can be expressed as,

$$A = 4\pi R^2 \qquad \text{(Eq. 2.5)}$$

The same amount of energy spreads out on an incremented spherical surface at an incremented spherical radius. That means: the power density on the surface of a sphere is inversely proportional to the radius of the sphere. So we get the formula to calculate the No directional Power Density S_u

$$S_u = \frac{P_s}{4\pi R_1^2} \quad [W/m^2] \qquad \text{(Eq. 2.6)}$$

P_S = transmitted power [W]

S_U = no directional power density,

R_1 = Range antenna to Target [m].

Since a spherical segment emits equal radiation in all direction (at constant transmit power), if the power radiated is redistributed to provide more radiation in one direction, then this results an increase of the power density in direction of the radiation. This effect is called antenna gain. This gain is obtained by directional radiation of the power. Sg, from the definition, the directional power density is:

$$S_g = S_u \cdot G \qquad \text{(Eq. 2.7)}$$

S_g = directional power density

G = antenna gain

The target detection is not only depends on the power density at the target position, but also how much power is reflected from the target. In order to determine the useful reflected power, it is necessary to know the radar cross section σ. This quantity depends on several factors.

But it is true to say that a bigger area reflects more power than a smaller area. With this in mind we can say: The reflected power P_r at the radar depends on the power density S_u, the antenna gain G, and the variable radar cross section σ:

$$P_r = \frac{P_s \cdot G \cdot \sigma}{4\pi R_1^2} \text{ [W]} \qquad \text{(Eq. 2.8)}$$

P_r = reflected power

σ = radar cross section

R1 = range antenna - target [m]

Simplified a target can be regarded as a radiator in turn due to the reflected power. In this case the reflected power P_r is the emitted power.

Since the echoes encounter the same conditions as the transmitted power, the power density yielded at the receiver S_e is given by:

$$S_e = \frac{P_r}{4\pi R_2^2} \quad [W/m^2] \qquad \text{(Eq. 2.9)}$$

S_e = power density at receiver

P_r = reflected power [W]

R_2 = range target - antenna [m]

At the radar antenna the received power depends on the power at the receiver P_E and the effective antenna area A_W.

$$P_E = S_e \cdot A_W \qquad \text{(Eq. 2.10)}$$

P_E = power at the receive place [W]

A_W = effective antenna area [m^2]

The effective antenna area arises from the fact that an antenna suffer from losses, therefore, the received power at the antenna is not equal to the input power. As a rule, the efficiency of the antenna is around 0.6 to 0.7 (Efficiency K_a).

Applied to the geometric antenna area, the effective antenna area is:

$$A_W = A \cdot K_a \qquad \text{(Eq. 2.11)}$$

A_W = effective antenna area [m²]

A = geometric antenna area [m²]

K_a = efficiency

The power received, P_E is then calculated:

$$P_E = S_e \cdot A_W \qquad \text{(Eq. 2.12)}$$

$$A_W = A \cdot K_a \qquad \text{(Eq. 2.13)}$$

$$P_E = S_e \cdot A \cdot K_a \qquad \text{(Eq. 2.14)}$$

$$P_E = \frac{P_r A K_a}{4\pi R_2^2} \text{ [W]} \qquad \text{(Eq. 2.15)}$$

The transmitted and reflected waves have been seen separately. The next step is to consider both transmitted and reflected power: Since R_2 (Target - Antenna) is the distance R_1 (Antenna - Target) then,

$$P_E = \frac{P_r A K_a}{4\pi R_2^2} \text{ [W]} \qquad \text{(Eq. 2.16)}$$

$$P_r = \frac{P_s G \sigma}{4\pi R_1^2} \text{ [W]} \qquad \text{(Eq. 2.17)}$$

$$P_E = \frac{P_s G \sigma A K_a}{(4\pi)^2 R_1^2 R_2^2} \text{ [W]} \qquad \text{(Eq. 2.18)}$$

$$R_1 = R_2 \qquad \text{(Eq. 2.19)}$$

$$P_E = \frac{P_s G \sigma A K_a}{(4\pi)^2 R^4} \quad [W] \quad \text{(Eq. 2.20)}$$

Another equation, which will not be derived here, describes the antenna gain G in terms of the wavelength λ.

$$G = \frac{4\pi A K_a}{\lambda^2} \quad \text{(Eq. 2.21)}$$

Solving for A, antenna area, and replacing A into equation 2.20, after simplification it yields

$$P_e = \frac{P_s G^2 \sigma \lambda^2}{(4\pi)^3 R^4} \quad [W] \quad \text{(Eq. 2.22)}$$

Solving for range R, we obtain the classic radar equation

$$R = \sqrt[4]{\frac{P_s G^2 \lambda^2 \sigma}{P_E (4\pi)^3}} \quad \text{(Eq. 2.23)}$$

All quantities that influence the wave propagation of radar signals were taken into account at this equation. For a given radar equipment most sizes (P_s, G, λ) can be regarded as constant since they are only variable parameters in very small ranges. The radar cross section, on the other hand, varies heavily but for practical purposes we will assume $1m^2$.

$$R_{max} = \sqrt[4]{\frac{P_s G^2 \lambda^2 \sigma}{P_{E\,min} (4\pi)^3}} \quad [m] \quad \text{(Eq. 2.24)}$$

The smallest received power that can be detected by the radar is called P_{Emin}. Smaller powers than P_{Emin} are not usable since they are lost in the noise of the receiver. The minimum power is detect at the maximum range R_{max} as seen from the equation 2.24. An application of this radar equation is to easily visualize how the performance of the radar units influence the range.

CHAPTER 3

ASSESSING NEEDS AND SPECIFICATIONS

In this chapter, the requirements for hardware and critical specifications are assessed, theoretically and empirically. The requirements for Doppler radar are considered from the relationship of signal and noise sources in the system. In order to assess the specifications of radar systems, free space loss, one way received signal power, and round trip received signal power are calculated and measured. Also in order to measure round trip received signal power, an effort was required to eliminate interference from direct coupling between the transmitting antenna and receiving antenna, or Tx signal leakage to the receiver chain. Those components have to be removed to measure accurate received signal power. In this chapter, a measurement technique for round trip received signal power with LO compensation technique is also shown.

3.1 Sensitivity Dependence

In a direct conversion doppler radar system, both the SNR in the RF band and SNR in the base band affect the sensitivity. All components in the system affect either SNR. Fig. 3.1 shows the signals and noise in the system. As described above, there are two SNR. For SNR in the RF band, adequate LO signal power is necessary. For accurate or long range detection, this output power should be as high as possible. The next component is the round trip loss. This component includes free space loss, radar cross section, and the antenna gain. Due to the

transmitted power and these round trip losses, the received signal power can be achieved. For SNR at RF, the phase noise affects to the noise floor. For base band signal, the conversion loss of the mixer defines the signal power of base band signal. Theoretically 4.5dB of conversion loss can be achieved by a passive mixer. For SNR at base band, the flicker noise is dominant.

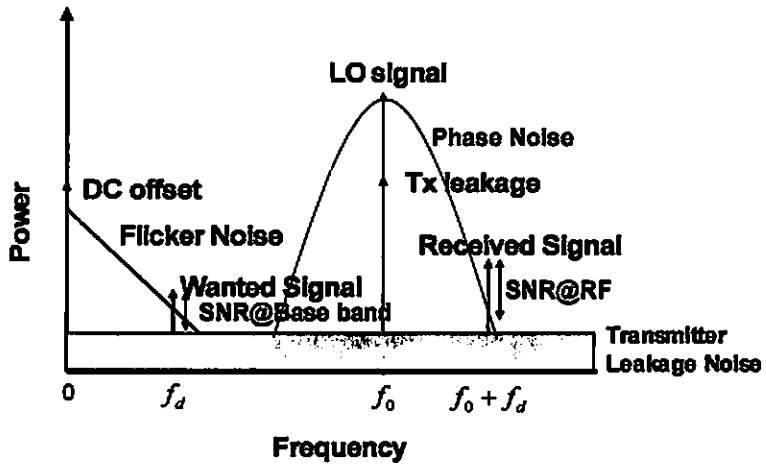

Fig 3.1. Signals and noise sources in the system

3.2 Free Space Loss

For radar sensing techniques, one of the most important factors is the free space loss at the frequency of the transmitted signal. The detection limits in a high frequency system significantly depend on the free space loss which represents how much the signal is attenuated through space. By calculating it, the range limitation can be roughly estimated.

The one way free space loss factor α_1 is given by the $\frac{4\pi R^2}{\lambda}$. As shown in figure3.2, the loss is due to the ratio of two factors (1) the effective radiated area of the transmit antenna, which is the surface area of a sphere $4\pi R$ at the distance R, and (2) the effective capture are A_e of receive antenna which has a gain of one. If a receiving antenna could capture the

whole surface area of the sphere, there would be no spreading loss, but a practical antenna will capture only a small part of the spherical radiation. Space loss is calculated using isotropic antennas for both transmit and receive, so α_1 is independent of the actual antenna. The value of the received signal (S) is:

$$P_r = \frac{P_t G_t G_r \lambda^2}{4\pi R^2} = P_t G_t G_r \left(\frac{\lambda^2}{4\pi R^2} \right) \qquad \text{(Eq. 3.1)}$$

To convert this equation to dB form, this is written as

$$10\log P_r = 10\log \frac{P_t G_t G_r \lambda^2}{4\pi R^2} = 10\log P_t G_t G_r \left(\frac{\lambda^2}{4\pi R^2} \right) = 10\log P_t G_t G_r + 10\log \left(\frac{\lambda^2}{4\pi R^2} \right)$$

$$= 10\log P_t G_t G_r + \alpha_1 \qquad \text{(Eq. 3.2)}$$

Where the one-way free space loss α_1 is defined as $10\log\left(\frac{\lambda^2}{4\pi R^2} \right)$.

From this equation, the free space loss for 2.4 GHz was calculated and shown in Fig. 3.3.

(a) Physical Concept

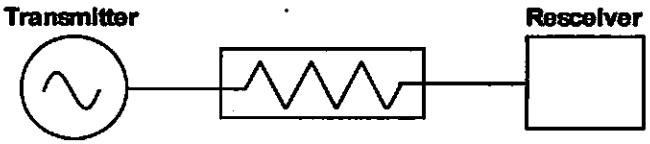

(b) The Equivalent Circuit

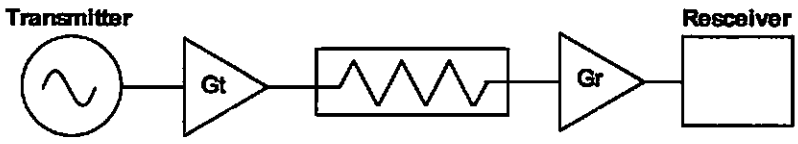

(c) The Equivalent Circuit with Antennas
Fig 3.2. Concepts for one way space loss

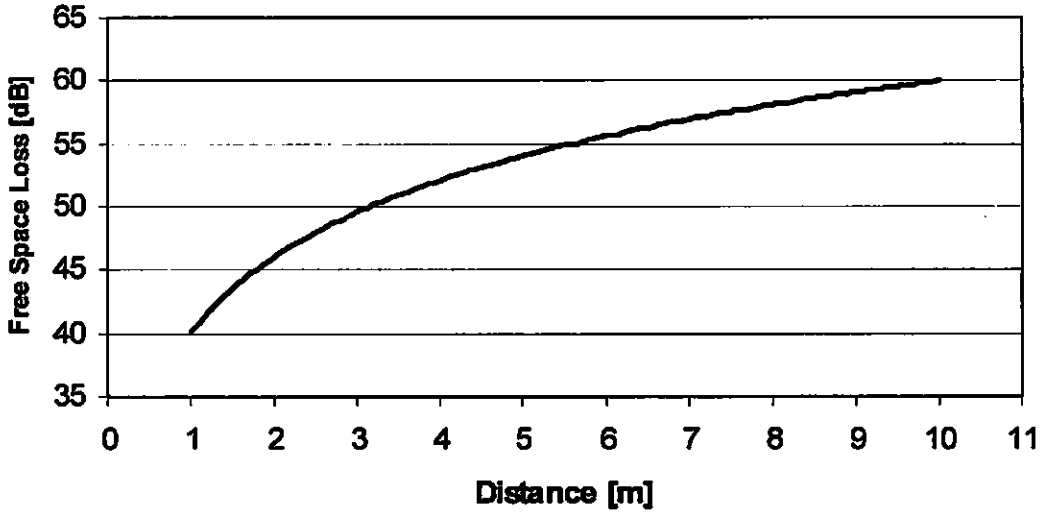

Fig. 3.3. Free space loss

3.3 Received Signal Power

3.3.1 One way

The one way received signal power represents how much transmitted signal power reaches the target. The expected reflected signal power can be estimated from this. From the one way radar equation shown below, the one way received signal power of the Doppler radar system is calculated and measured. The one way radar equations is

$$P_r = \frac{P_t G_t G_r \lambda^2}{(4\pi R)^2} \qquad \text{(Eq. 3.3)}$$

Where P_t is transmitted signal power, G_t and G_r are antenna gain of transmitting and receiving antenna, R is the range between two antennas. Fig. 3.4 shows the measurement setup for one way received signal power. In this measurement, 0dBm of transmitting power was used. For both antennas, antenna specialist ASPPT2988 which has 8dBi of Antenna

Gain was used face to face. Fig. 3.5 shows the measurement results and theoretical results. From this result, the target can receive -24dBm of signal power at the 1m case which normally used for heart beat detection measurement was achieved.

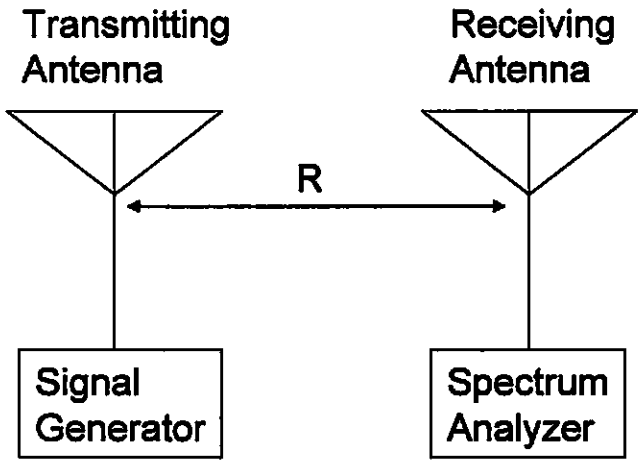

Fig. 3.4. The measurement setup for one way received signal power

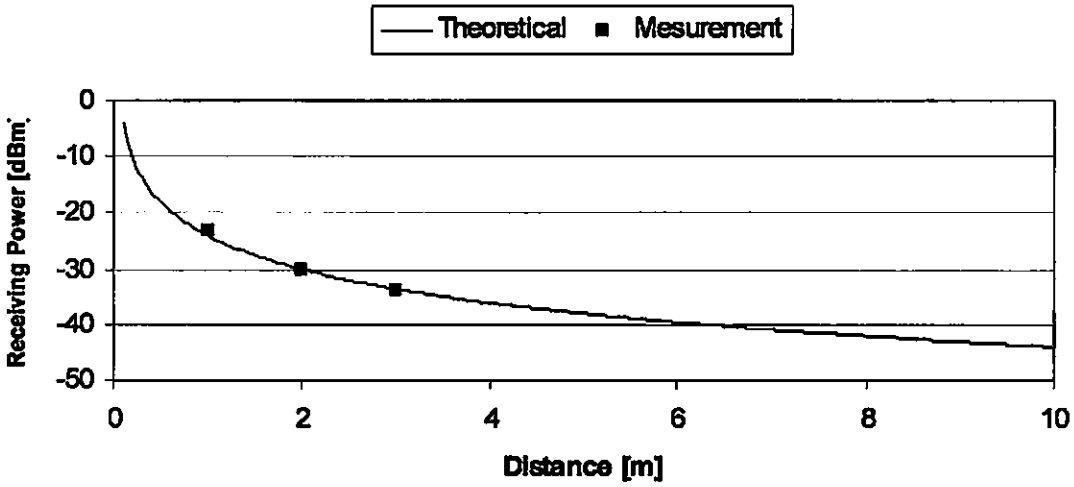

Fig. 3.5. Theoretical and measured results of one way received signal power

3.3.2 Round Trip

From one way received signal power, the round trip received signal can be calculated, which is the most important information for assessing the limitations for a system. From the radar equation, the round trip received signal power of a Doppler radar system can be calculated and measured. The round trip radar equations is

$$P_r = \frac{P_t G_t G_r \lambda^2 \sigma}{(4\pi)^3 R^4} \qquad \text{(Eq. 3.4)},$$

where P_t is transmitted signal power, G_t and G_r are antenna gain of transmitting and receiving antenna, R is the range between two antennas, and σ is the radar cross section of the target. There is the problem in order to measure the reflected signal power. For the transceiver configuration, the LO leakage from the circulator, and the multiple antenna system has the direct coupling between the transmitting and the receiving antenna. Therefore a compensation technique is required to measure the received signal power. In order to measure received signal power, a direct coupling compensation technique was used with multiple antenna system and the measurement set up shown in Fig. 3.6. In order to compensate, the LO signal is split by a power splitter and one is for transmitting, and another is to compensate the direct coupling signal. For compensation, the separated signal is attenuated and the phase is adjusted in order to make 180 degree phase difference from the direct coupling signal. Then the two signals were added to power combiner, and the signals compensate each other. After eliminate the direct coupling signal, a reflector was putted in front of the both antenna to make signal reflection. By doing this compensation technique, only reflected power can be measured accurately. For the calculation and the measurement,

0dBm of transmitted signal power, 8dBi of antenna gain, 0.125m of λ, and 0.09cm^2 of the radar cross section were used. Fig. 3.7 shows the theoretical and measured results.

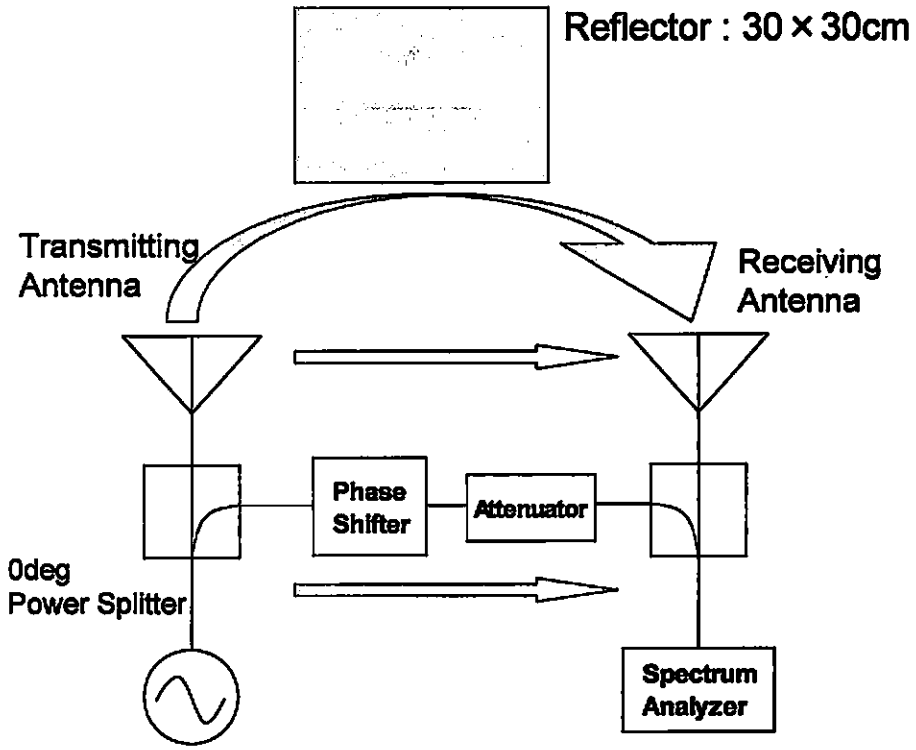

Fig. 3.6. Measurement setup for round trip received signal power

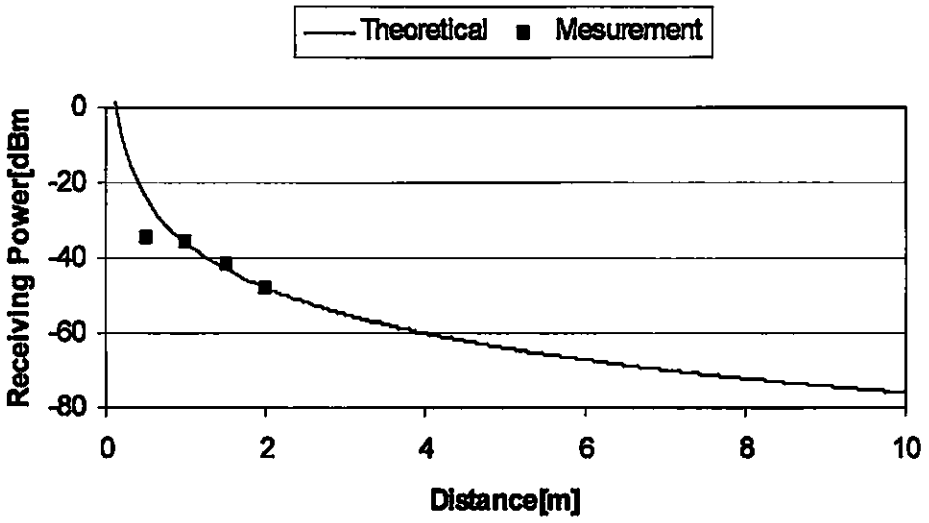

Fig. 3.7. Theoretical and measured results of round trip received signal power

3.4 Various Transmitted Signal Power Measurements

According to range correlation theory, performance limits in Doppler radar sensing depend on the phase noise and amplitude modulation noise sidebands of the local oscillator signal. In this section, heart rates were measured using a Doppler radar system with incrementally reduced transmit power levels in order to assess the lower limits for system performance. Measurements were made both for subjects holding their breath and for subjects breathing normally, with the former used to assess absolute performance limits for the radar circuit, and the latter used to asses the secondary impact resulting from the more complex chest motion. The power of the received signal in a Doppler radar system can be affected by many parameters including transmit power level, path obstructions, target composition and cross section, and antenna patterns. In this work, only transmit power was varied with all other parameters held constant by using an attenuator used to incrementally decrease the transmitted signal. The measurement setup for the low power measurements is shown in Fig. 3.8.

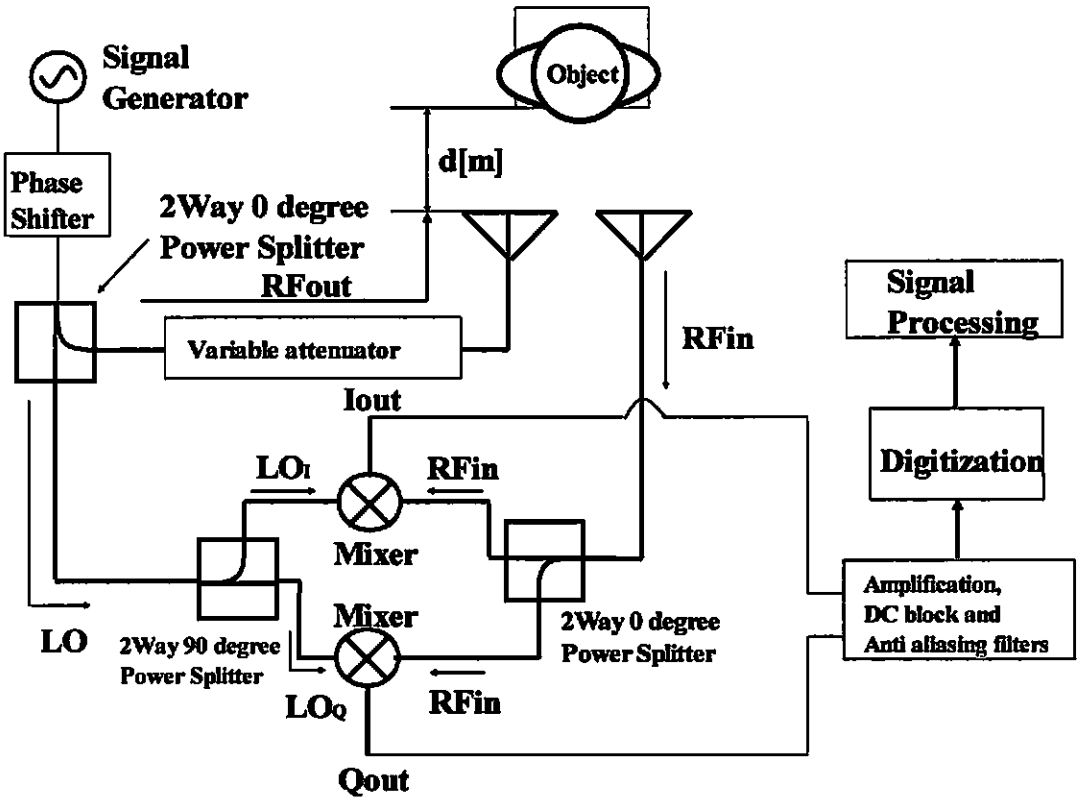

Fig. 3.8. Measurement setup for variable transmitted signal power

The external signal source was set to 11 dBm in order to get a 0 dBm LO-input power for the mixer. While the ideal LO power for the mixer is 7 dBm, a 0dBm signal was used for this measurement to maintain circuit simplicity. The conversion loss of the mixer is 5.4dB at a 7dBm LO power, and 7.26dB at a 0 dBm LO power. This implies that the measured system limits might still be improved. Two variable attenuators were used to incrementally reduce the RF output power. Each attenuator provided 0 to 30 dB attenuation in 1 dB steps. In order to compensate for the phase change introduced by each different attenuator settings, a compensating phase shifter was introduced after the signal generator. With this, the phase change introduced with each increment of the attenuator could be completely compensated. Another phase shifter was also used to further optimize the phase to avoid null points. The baseband output signals were amplified and filtered with SR560 LNAs and then digitized

with a Tektronix 3014 digital oscilloscope. A wired finger pressure pulse sensor was used as a reference for comparison with the heart rate data obtained with the Doppler radar. A peak detector and digital band pass filter implemented in MATLAB were used for signal processing for signals under both breath-hold and normal conditions.

When the subject breathes during a measurement, there is some phase variation and resulting frequency distortion, as described in [5]. To avoid this impacting rate detection accuracy, the subject did not breathe during the initial measurements. The result for the system operating at 2 mW is shown in Fig. 3.9. The plot indicates an average beat-to-beat interval of about one second, with expected agreement between finger-pulse reference and radar results. The result for 0.2 μW is shown in Fig. 3.10. At this point the system still functions well, with no discernable degradation. A second plot at this power level is also shown (Fig. 3.11), also indicating close agreement with reference measurements in spite of the additional phase modulation effects introduced by respiration related chest motion.

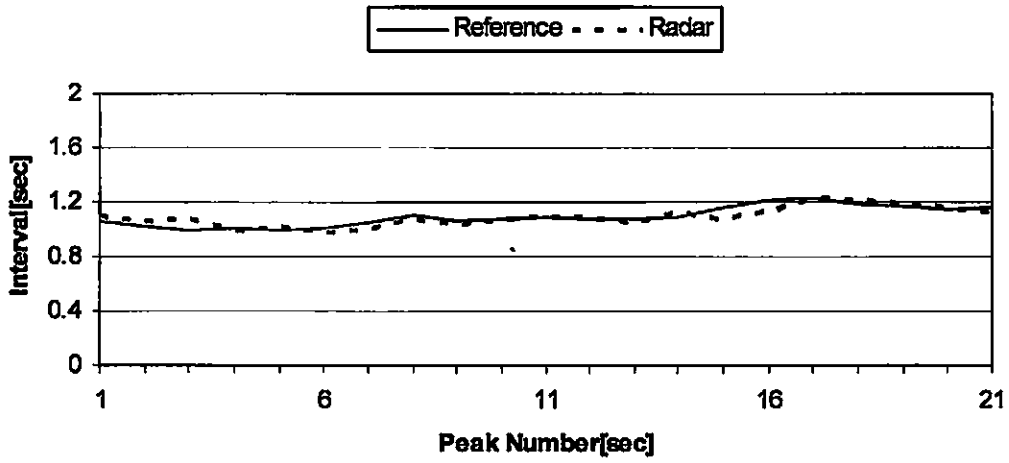

Fig. 3.9. Measured results at 2mW, without respiration.

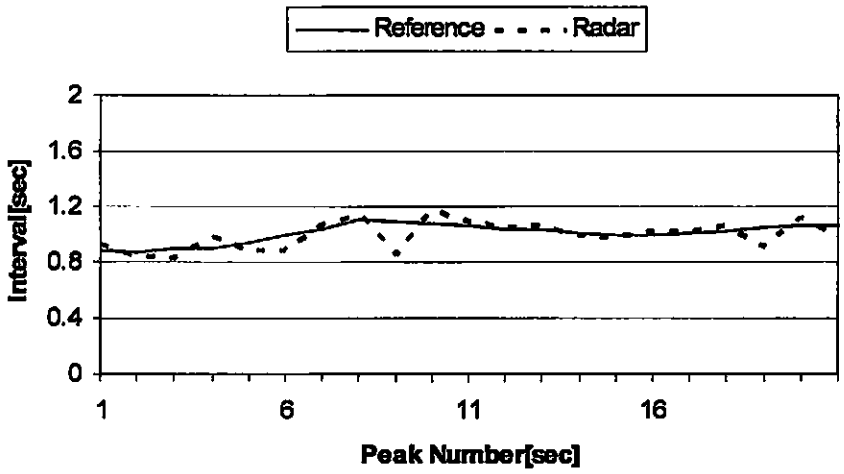

Fig. 3.10. Measured results at 0.2μW, without respiration.

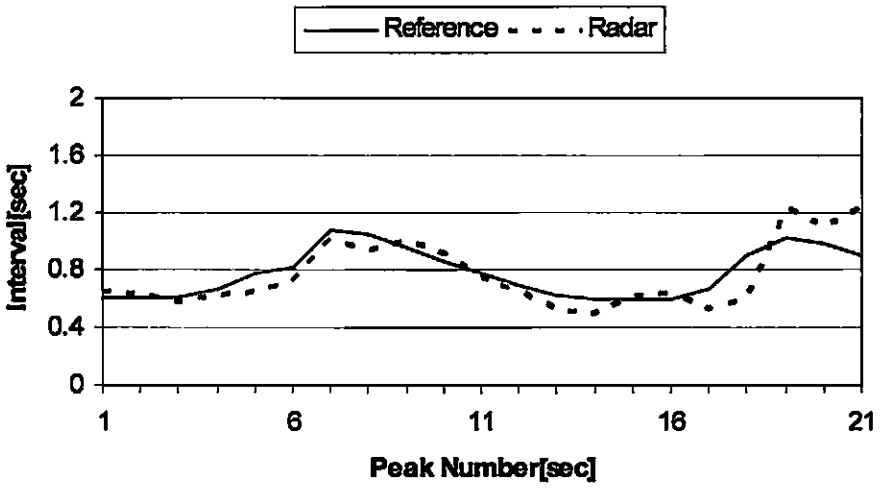

Fig. 3.11. Measured result at 0.2μW, with respiration.

The measured results for 20 nW is shown in Fig. 3.12. Here appreciable degradation can be observed in the rate tracking for the Doppler radar signal. Still, the rate is tracked with reasonable accuracy and may be useful for many applications.

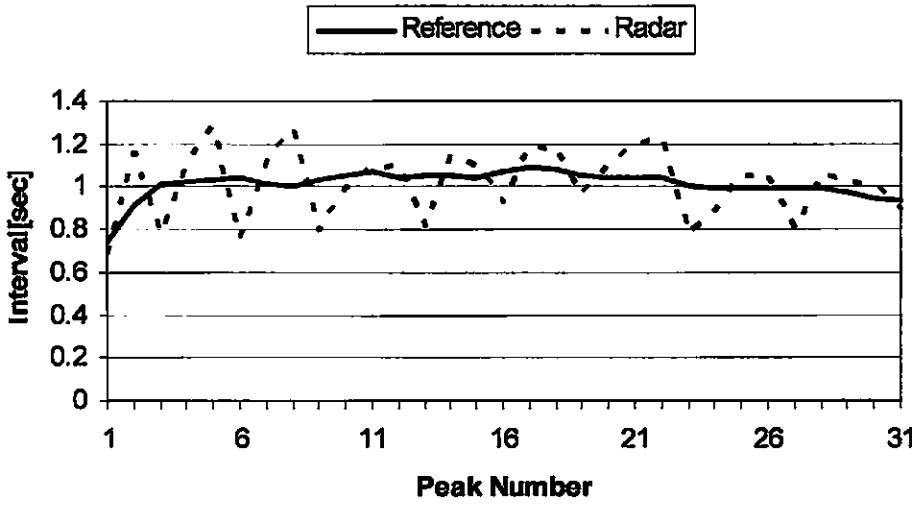

Fig. 3.12. Measured results at 20 nW, without respiration.

In Fig. 3.13, average amplitude of base band signal for various transmitted signal power levels, and corresponding mean square error are shown.

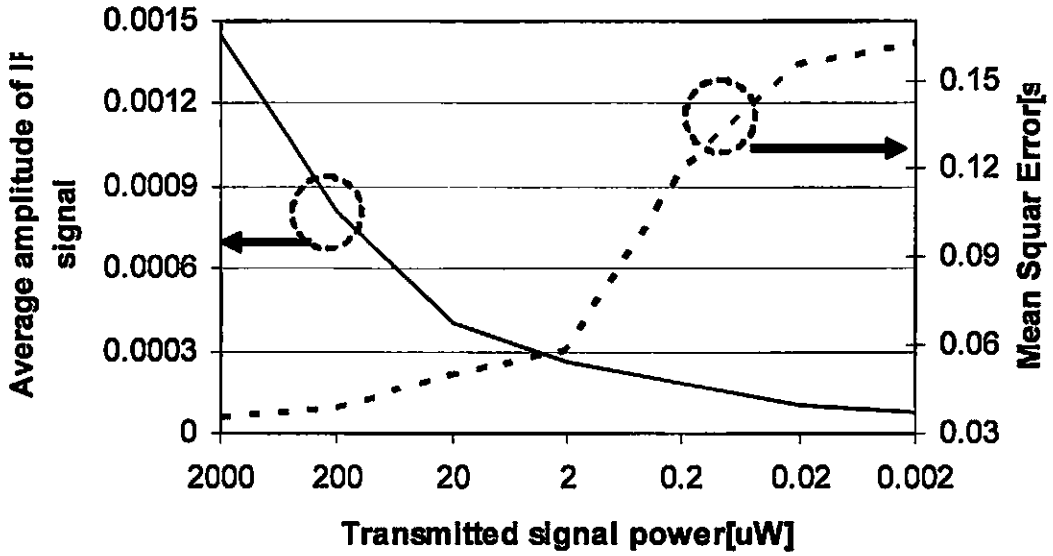

Fig. 3.13. Average amplitude of baseband signal for various transmitted signal power levels, and corresponding mean square error

CHAPTER 4

CIRCUIT DESIGN FOR IMPROVED PERFORMANCE

4.1 Circuit Design

4.1.1 Direct Conversion System

Down- or up- conversion can be roughly divided into two two methods. One is heterodyne systems, and the other is homodyne systems. For a heterodyne system, a high frequency filter is required for frequency down conversion, because unwanted signals such harmonics and spurious noise come from the down converting process. For instance, in a cell phone receiver front end, a filter which has high Q-factor is required to avoid image interference. However, such a filter is expensive and physically large with respect to the system. Also it is hard to make a high Q filter on a silicon wafer. Therefore it is difficult to fabricate such an IC. In order to avoid such disadvantages of the heterodyne system, a direct conversion system ican be useful. In Fig. 4.1, the block diagram of direct conversion receiver is shown.

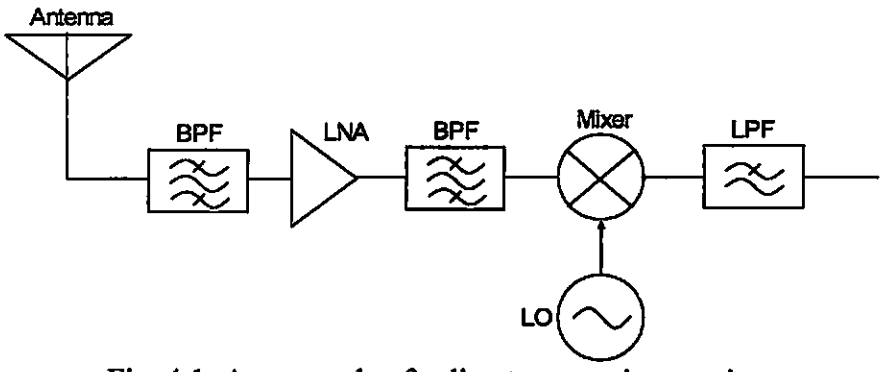

Fig. 4.1. An example of a direct conversion receiver

This method converts the received RF signal to base band signal directly. Therefore this method can eliminate the high frequency filters and make the system small size. However there are some disadvantages to use this system. First, the sensitivity of the receiver may get worth by the affect of IMD2 and IMD3 of the mixer. If there are some spurious in LO signal or RF signal, the IMD2 show up in low frequency which is near the base band signal, and interfere the detection. Second is the DC offset. The LO signal leaking from mixer may be reflected by other components, and if it inputted to mixer again, it makes second harmonics signal ($f_{LO}+f_{LO}$) and DC offset ($f_{LO}-f_{LO}$). The second harmonics $2f_{LO}$ can be eliminated by LPF, but the DC offset is outputted and it induces the flicker noise. This flicker noise directly affects to the sensitivity limitation of the system. Third is the leaking of Tx signal. If the LO to RF isolation of the mixer is poor, the LO signal is leaked from RF port and it is radiated by the antenna. In this research, several types of Doppler radar system were used and designed. However the basic circuit of those systems is this direct conversion system, and by using this method, heart beat and respiration rates were measured and describe. From next section, the design and measured results of Doppler radar system is described.

4.1.2 Quadrature Output Direct Conversion Transceiver

In Fig. 4.2, the block diagram of a quadrature output direct conversion Doppler radar transceiver is shown. The configuration is almost same as a basic direct conversion system which is shown in Fig. 4.1. The difference is that this configuration has two outputs which are I (Inphase) and Q (Quadrature phase) outputs to avoid detection null points. The manner in which the mixer output in a direct conversion Doppler radar is related to the target motion is known to be acutely dependent on the nominal target distance. The simplest case of direct

proportionality results for an "optimum" position that occurs periodically for displacements of $\pi/2$, with correspondingly distorted conditions occurring near the "null" positions in between. The use of a system with both in-phase (I) and quarature (Q) mixer output channels provides a means for avoiding null case measurements either through channel selection or appropriate combination.

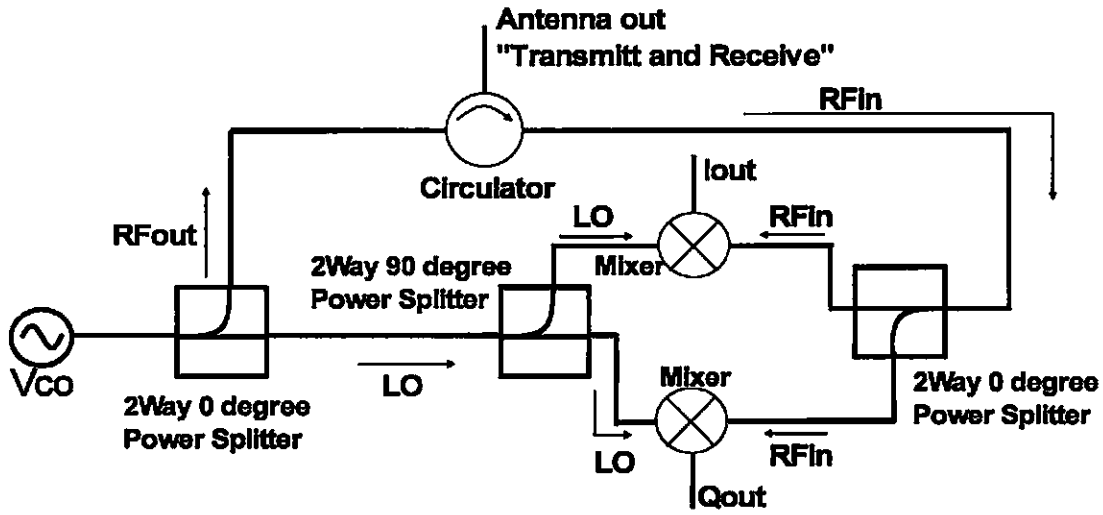

Fig. 4.2. Block Diagram of the Doppler Radar Transceiver

In this configuration, the signal of signal source were divided first by a two-way 0° power splitter (Mini-Circuits RPS-2-30) to separate the LO and RF output signals. The latter signal was directed to the transmit patch antenna through the circulator (Nova Microwave 0240CAD). This circulator separates transmitting and receiving chain. The former signal further divided by on-board two-way 90° power splitters (Mini-Circuits QCN-27) to make quadrature outputs. The radiated signal reflected by the subject was received by the same antenna to create the RF input signal, which was divided using a two-way 0° power splitter to feed the two receiver chains. Each chain had its own mixer (Mini-Circuits SKY-42) and produced the separate output channel signals as I_{out} and Q_{out} at the corresponding SMA connectors.

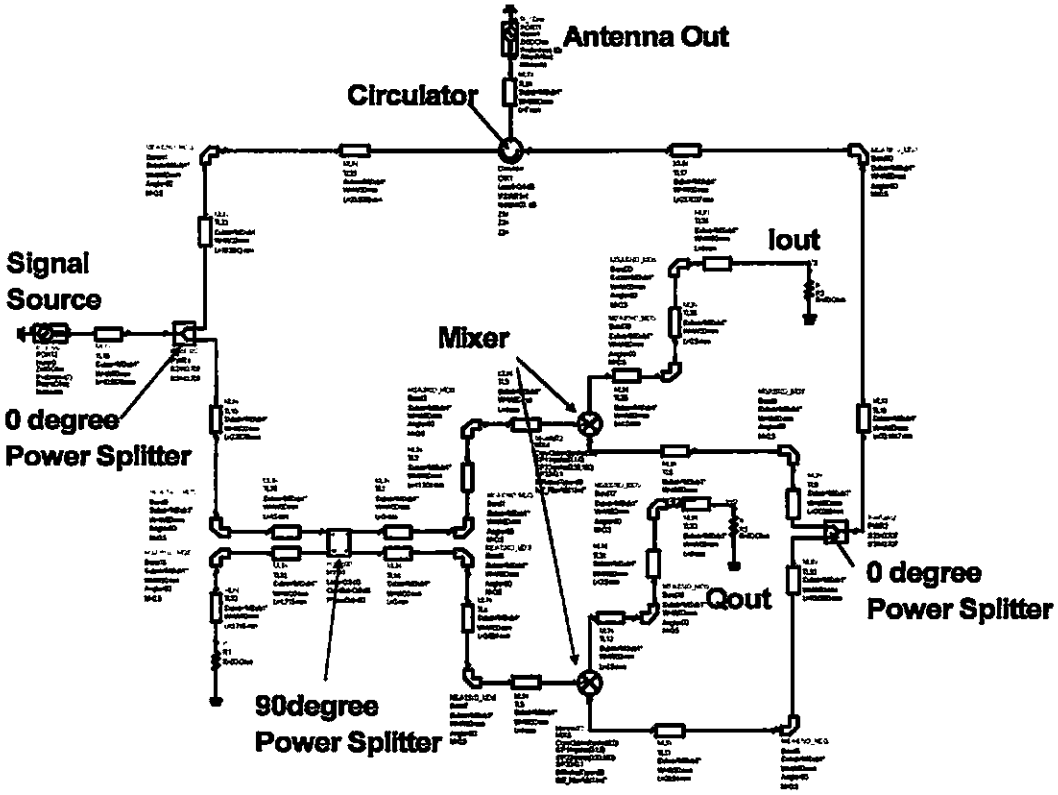

Fig. 4.3. The Schematic of Doppler Radar Transceiver

In Fig. 4.3, the circuit schematic of Doppler Radar Transceiver for I/Q imbalance simulation is shown. In Fig. 4.4, the phase difference of I and Q out simulation results are shown. From this simulation, the phase difference was 90.542 degree. For this configuration, an integrated system on a printed circuit board was designed and fabricated. The RF and LO signals flow via 50[ohm] microstrip lines and the design frequency is 2.4[GHz]. FR4 substrate is used for this board with the dielectric constant of 4.5, the substrate thickness of 1.57[mm], the conductor thickness of 0.035[mm], the metal conductivity of 5e7[s/m], and the tangent delta of 0.018. The board has a size of 101.6[mm] by 111.6[mm]. The VCO, Mini-Circuits JTOS-2700V, was used as a signal source, which delivers -4.67[dBm] at 2.4[GHz] signal to the

Antenna out, and consumes 70[mW]. In Fig. 4.5, the layout of Doppler Radar Transceiver is shown.

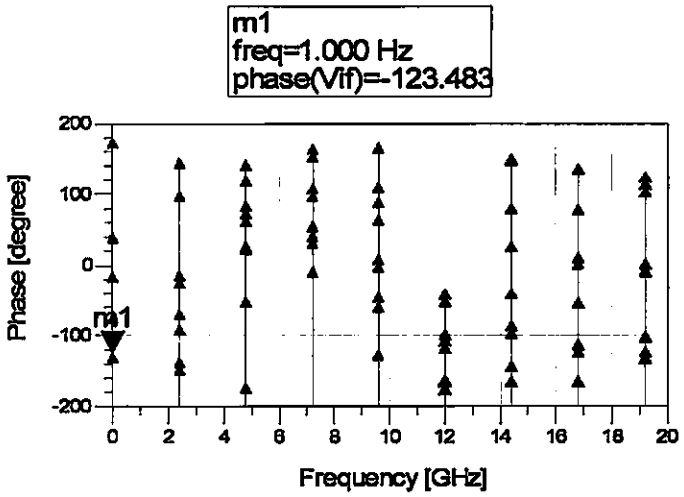

a) Iout

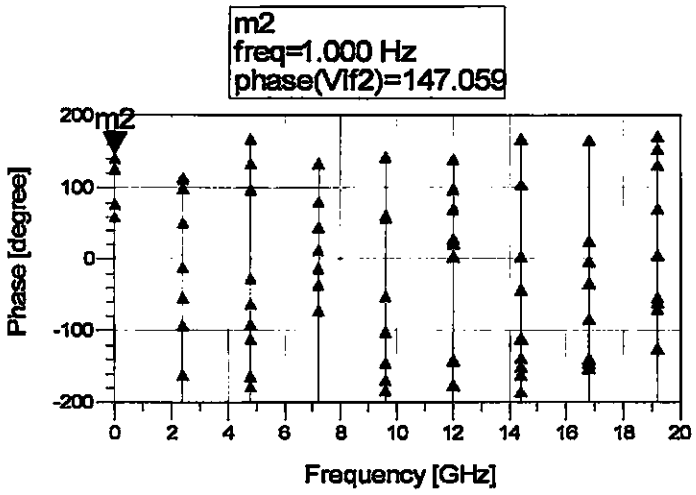

(b)Qout

Fig. 4.4. Phase Simulation Results

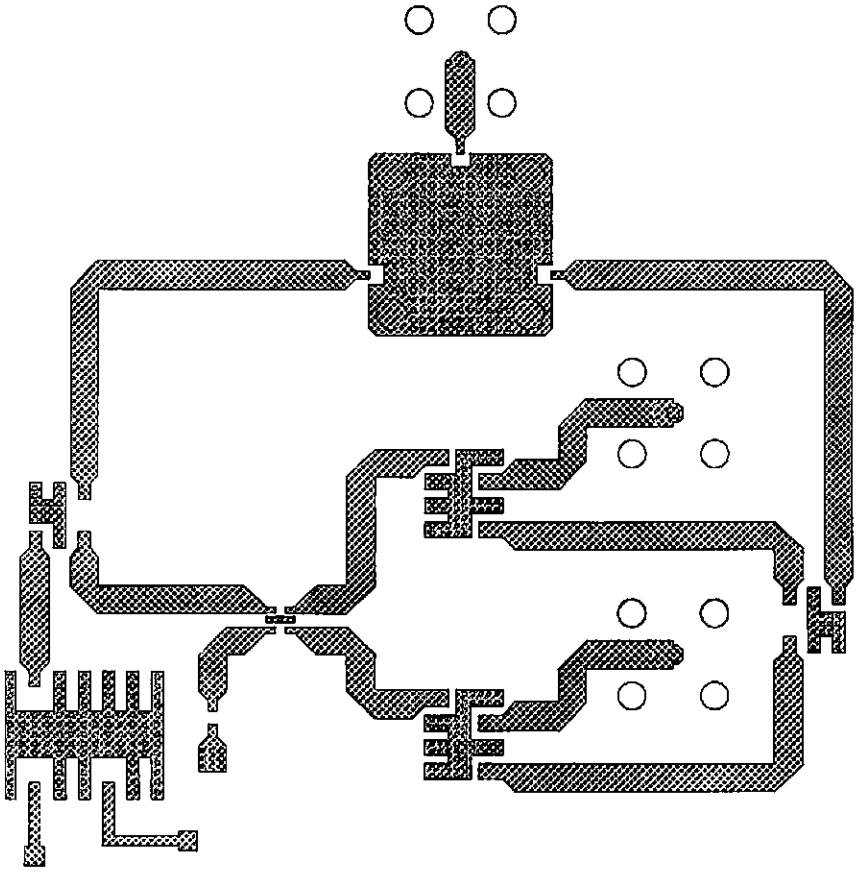

Fig4.5 The layout of Doppler Radar Transceiver

4.1.3 Multiple Antenna Doppler Radar System

In Fig. 4.6, the block diagram of a multiple antenna Doppler Radar system is shown. In order to detect cardiopulmonary activity for multiple people or detect a target in more than two dimensions, this configuration is designed and used. In this design, the circuits were divided into two parts. One is an LO feed circuit which delivers the LO signal to the Transmission chain and LO chain. The other is the quadrature direct conversion receiver circuit which receives the LO signal from the LO feed circuit and RFin signal delivered from

the receiving antenna. With this system, it is easy to increase the number of receivers when the observer wants to measure two or more people's heart rates, In this configuration, the signals were divided first by a two-way 0° power splitter (Mini-Circuits RPS-2-30) to separate the LO and RF output signals. The latter signal was directed to the transmit patch antenna, with the former signal further divided by on-board two-way 90° power splitters (Mini-Circuits QCN-27) to make quadrature outputs. The radiated signal reflected by the subject was received by the receiving patch antenna to create the RF input signal, which was divided using a two-way 0° power splitter to feed the two receiver chains. Each chain had its own mixer (Mini-Circuits SKY-42) and produced the separate output channel signals as I_{out} and Q_{out} at the corresponding SMA connectors.

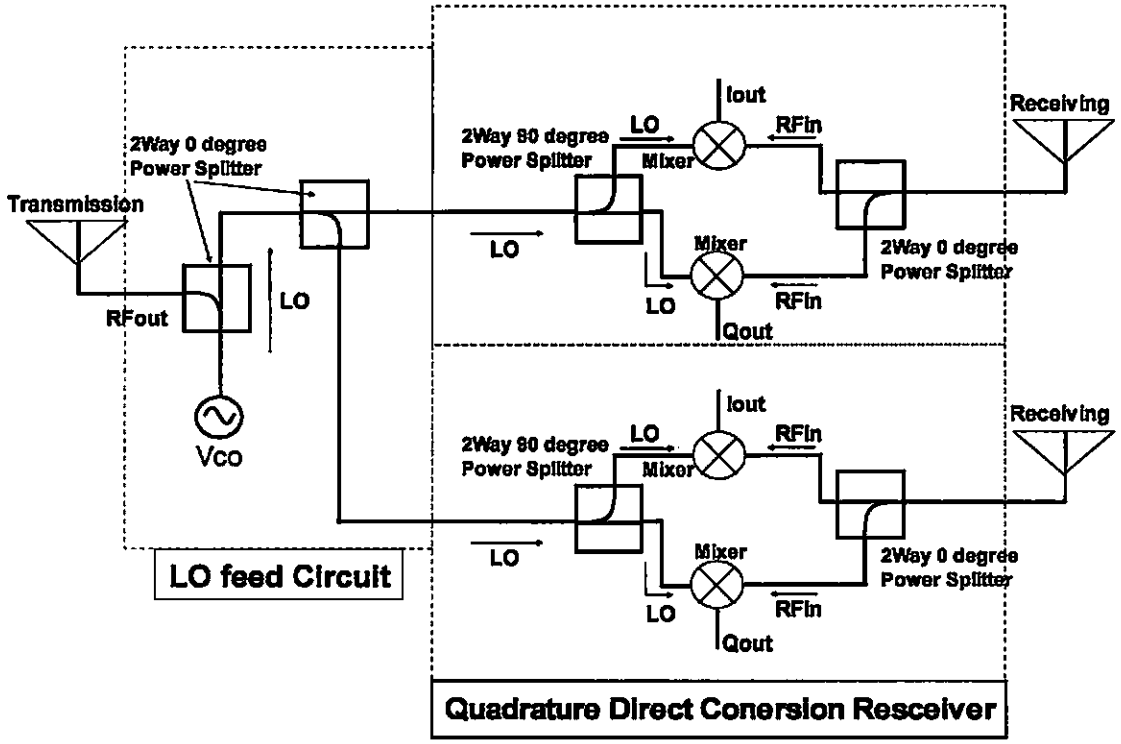

Fig. 4.6. Block Diagram of a multiple antenna system

Fig. 4.7 shows the circuit schematic of multiple target detection system and Fig. 4.8 shows the simulation results

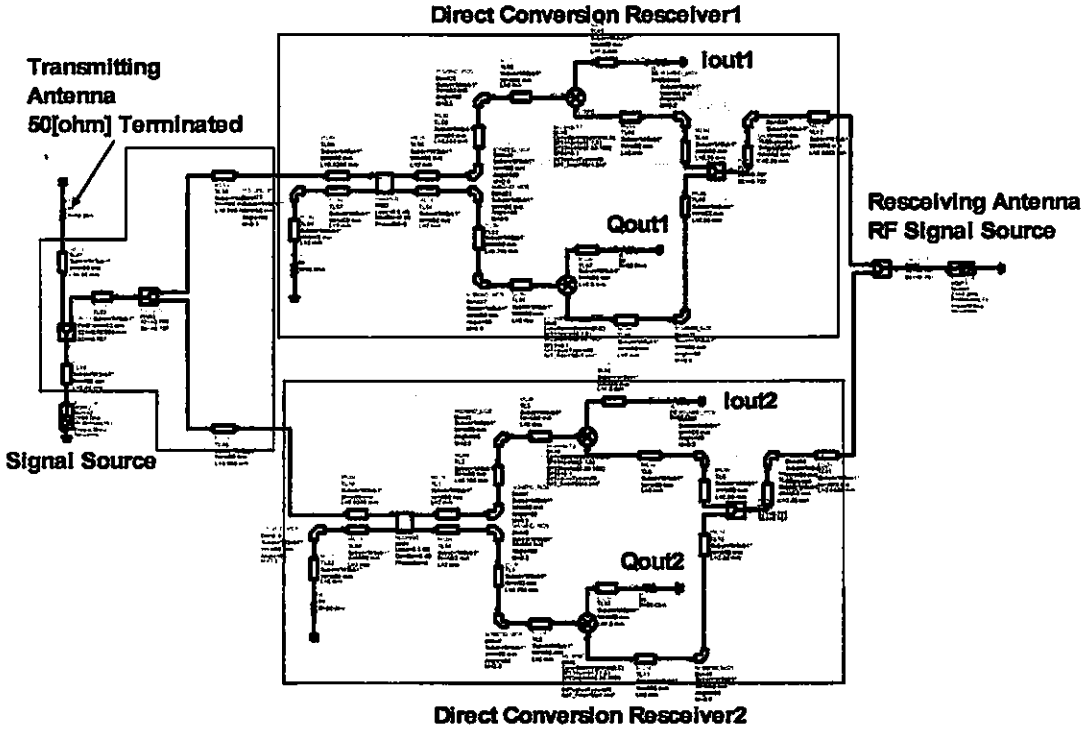

Fig. 4.7. The circuit schematic of SIMO Doppler Radar system

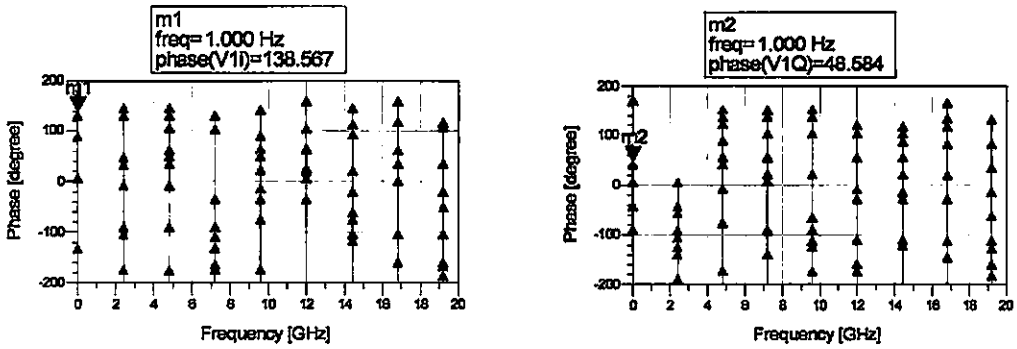

(a) Phase of Iout (b) Phase of Qout

Fig. 4.8. Phase simulation results for the multiple antenna system

Fig. 4.9 and 4.10 shows the Layout of direct conversion receiver and LO feed circuit. The RF and LO signals were routed via 50 Ω microstrip lines and the design frequency was 2.4 GHz.

An FR4 substrate is used for the PC board with a dielectric constant of 4.5, a substrate thickness of 0.787 mm, a conductor thickness of 35μm, a metal conductivity of 5.5e7 S/m, and a delta loss tangent of 0.018. These circuits were fabricated as a compact microstrip circuit with surface mount components on a 3-cm by 4-cm PC board, with coaxially connected commercial patch antennas (Antenna Specialists ASPPT2988 2.4 GHz) and an external Agilent 83640B signal source.

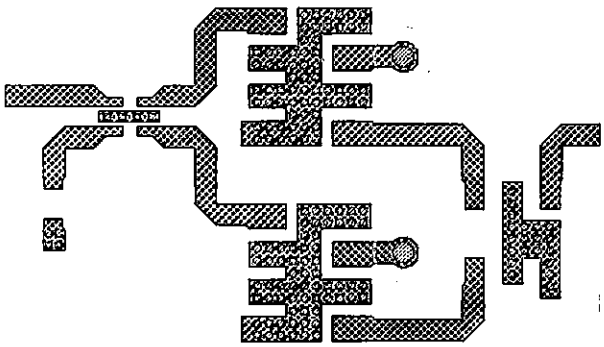

Fig. 4.9 Quadrature direct conversion receiver

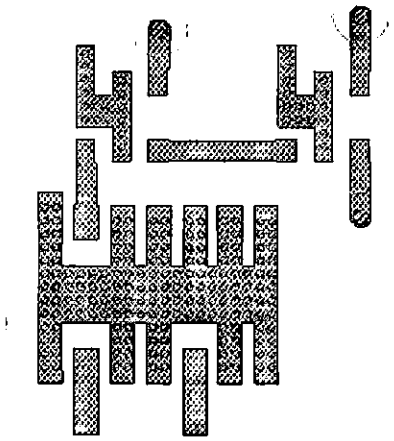

Fig. 4.10 LO feed circuit with VCO

4.2 Fabrication and Measurement

4.2.1 The Doppler Radar Transceiver

A photograph of the fabricated quadrature direct conversion circuit is shown in Fig. 4.11. Fig. 4.12 shows the measured amplitude and phase imbalance between I and Q channels. The amplitude imbalance was 4.7, phase imbalance was 18.5 degrees.

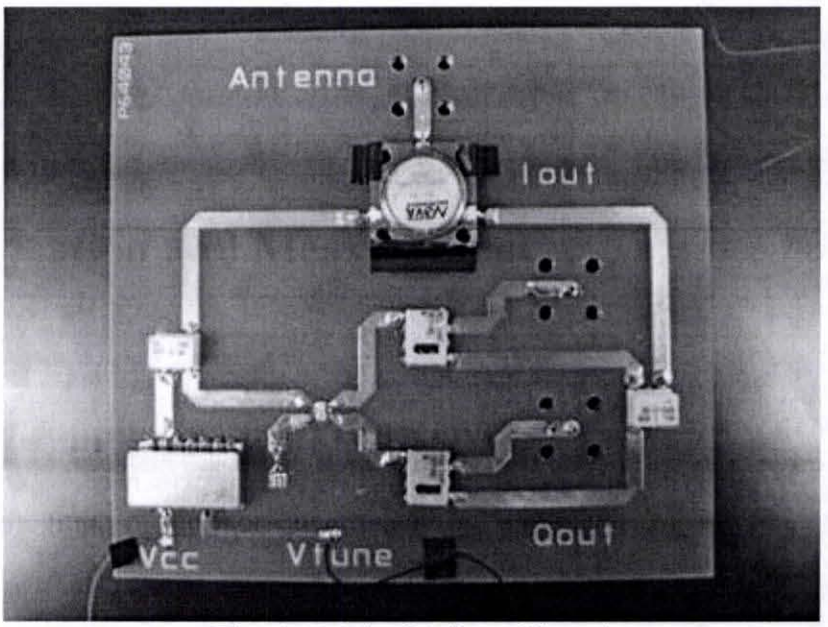

Fig. 4.11. The fabricated board

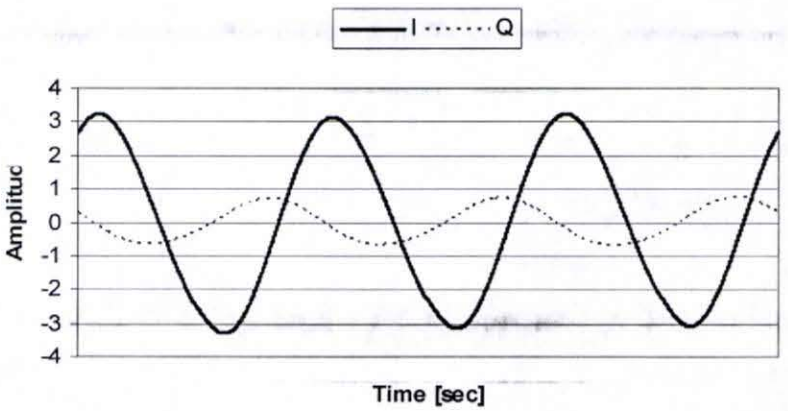

Fig. 4.12 Measured results of the imbalance factor of I and Q

In Fig. 4.13, the measurement setup for heart rate is shown. An HP E3630A was used as the voltage source. It was biased from 5[V] to Vcc, and 8.866[V] was used to Vtune of the Vco in order to get a 2.4[GHz] signal. The baseband output signals were amplified and filtered with SR560 LNAs and then digitized with a Tektronix 3014 digital oscilloscope. A wired finger pressure pulse sensor was used only as a reference to compare with the heart rate data obtained with the Doppler radar. A commercially available Antenna Specialists ASPPT2988 2.4[GHz] ISM-band patch antenna was used. From Fig. 3.9, the heart rate trace data which is pink color trace corresponds the finger reference data trace. Therefore this transceiver board detects the target's heart beat well.

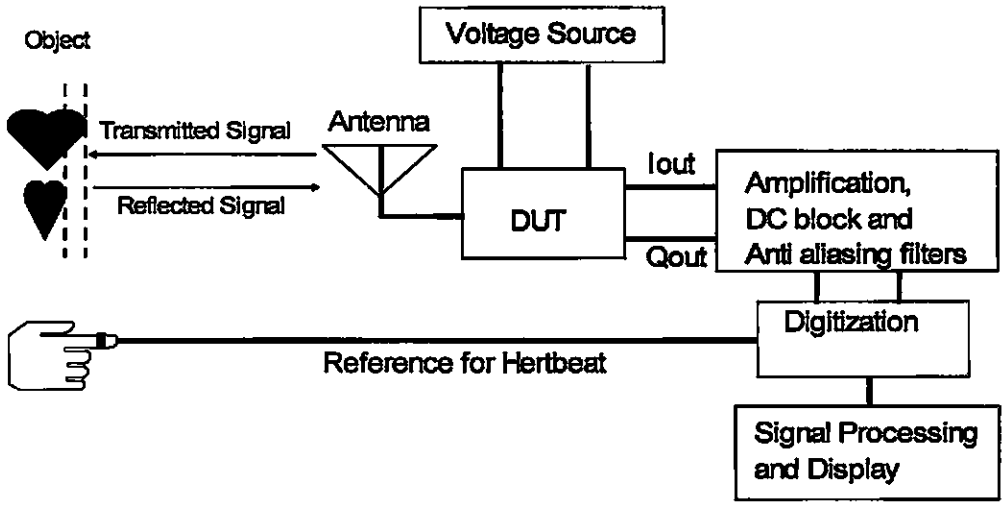

Fig. 4.13. Measurement setup for heart beat measurement

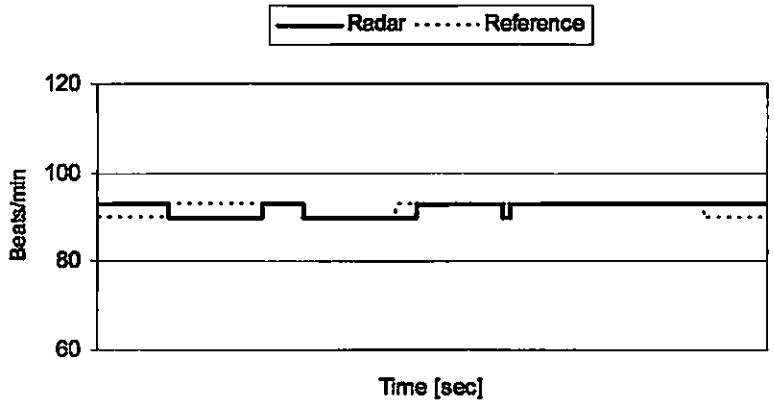

Fig. 4.14. Measured result of heart beat

4.2.2 Multiple Antenna Doppler Radar System

A photograph of the fabricated quadrature direct conversion circuit is shown in Fig. 4.15. Fig. 4.16 shows the measured amplitude and phase imbalance between I and Q channel. The amplitude imbalance was 0.25, phase imbalance was 6.48 degrees. Fig. 4.17 shows a photograph of fabricated LO feed circuit with Vco and Table 4.14 shows the measured results of output power from LO feed.

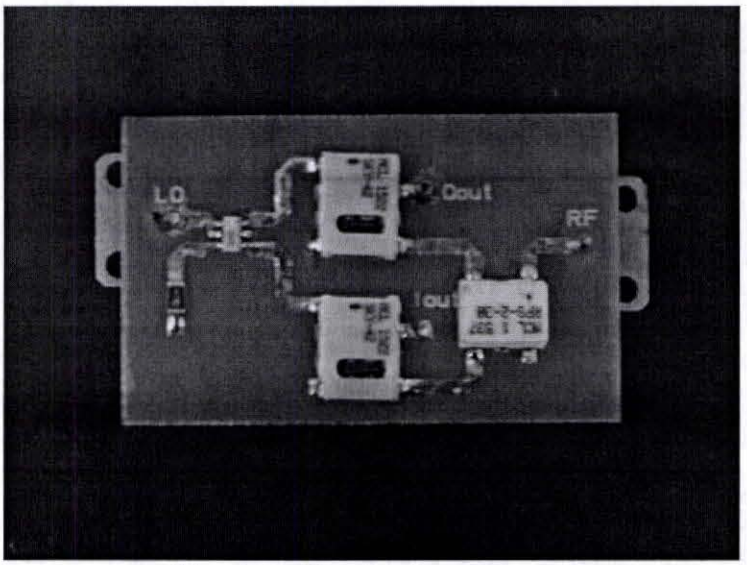

Fig. 4.15. The fabricated board

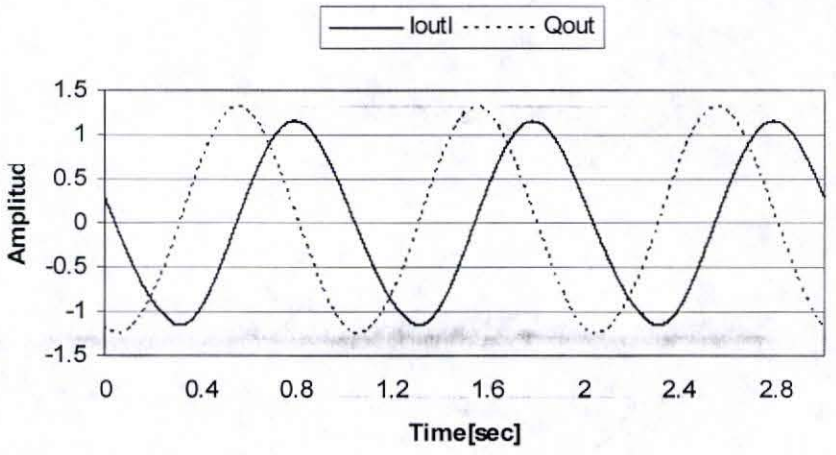

Fig. 4.16 Measured results of the phase difference of I and Q

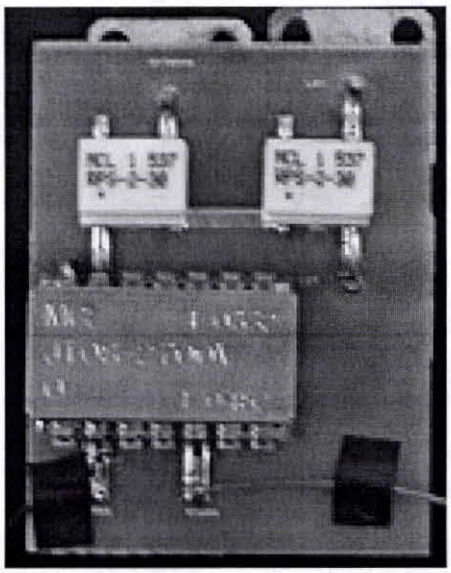

Fig. 4.17. Photograph of the fabricated board

Table 4.1 Measured results of LO feed circuit

	Antenna Out	LO1 out	LO2 out
Output Power[dBm]	3.41	-0.4	-0.6

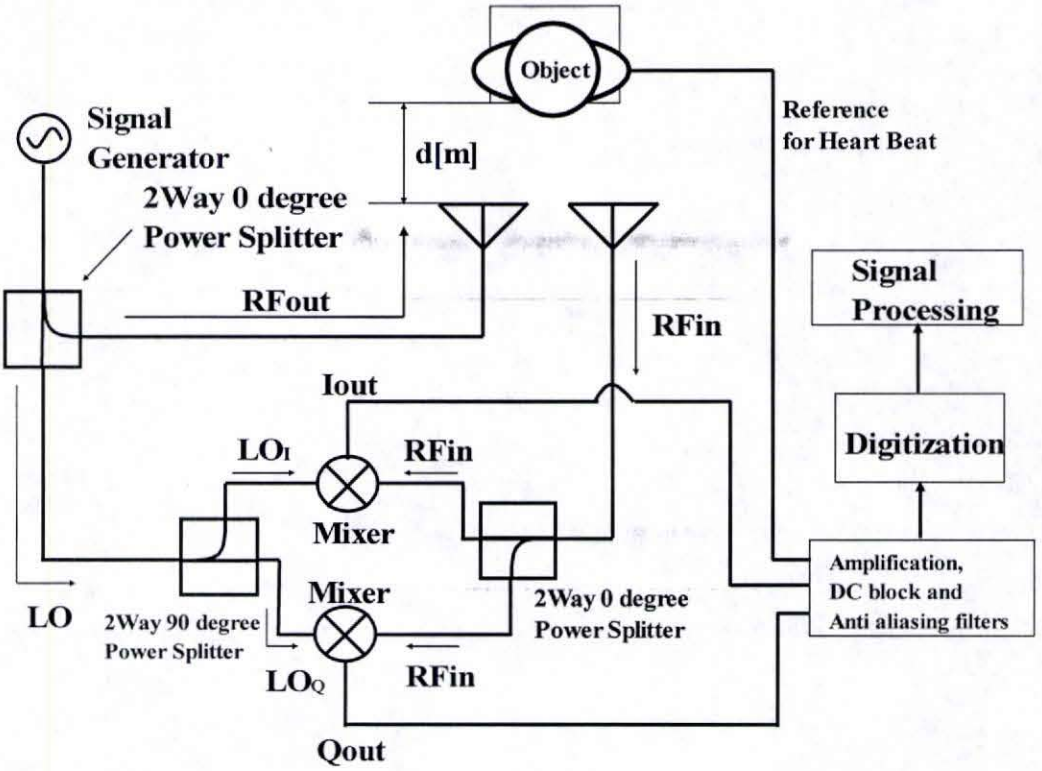

Fig. 4.18. Measurement setup for Heart beat detection

In Fig. 4.18, the measurement setup for heart rate detection is shown. The external signal source was set to 11 dBm in order to get a 0 dBm LO-input power for the mixer. While the ideal LO power for the mixer is 7 dBm, a 0dBm s ignal was used for this measurement to maintain circuit simplicity. The conversion loss of the mixer is 5.4dB at a 7dBm LO power, and 7.26dB at a 0 dBm LO power. This implies that the measured system limits might still be improved. The baseband output signals were amplified and filtered with SR560 LNAs and then digitized with a Tektronix 3014 digital oscilloscope. A wired finger pressure pulse sensor was used as a reference for comparison with the heart rate data obtained with the Doppler radar.

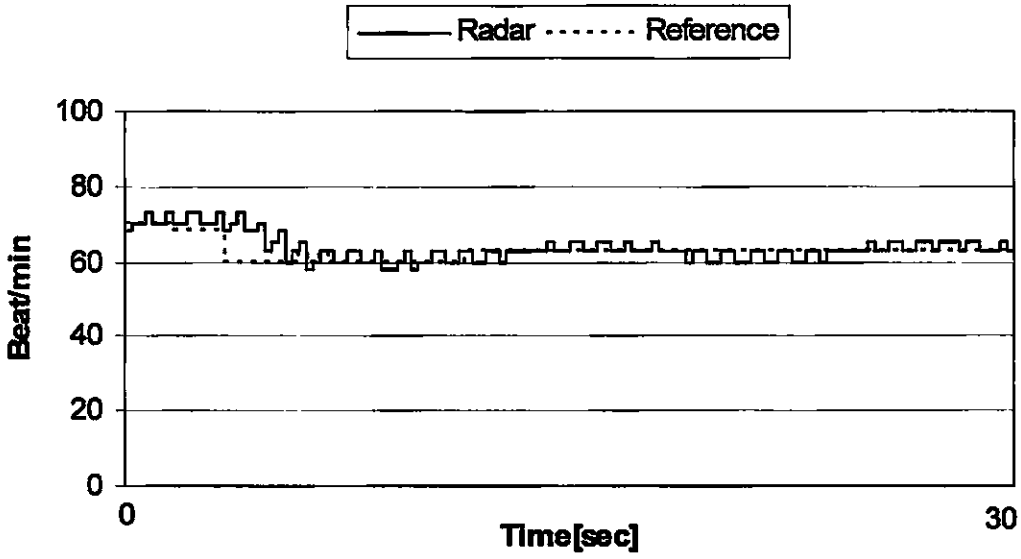

Fig. 4.19 Measured results of heart rate

CHAPTER5

ISSUES AND IMPROVEMENT FOR HARDWARE

5.1 Issues

5.1.1 Tx Leakage

As described above, the direct conversion transceiver configuration has several disadvantages, and one problem for heart rate sensing is Tx leakage to the Rx chain because of poor Tx to Rx isolation (Fig. 5.1). In the circulator configuration, to separate RFout pass and RFin pass, a circulator was used. The RFout signal is transmitted by antenna through circulator. The RFin signal is received by the same antenna and sent to the Rx chain through the circulator. In an actual system, the Tx signal can go through the circulator and directly reach Rx chain. In Fig. 5.2, the isolation characteristics of coaxial and surface mount circulators are shown.

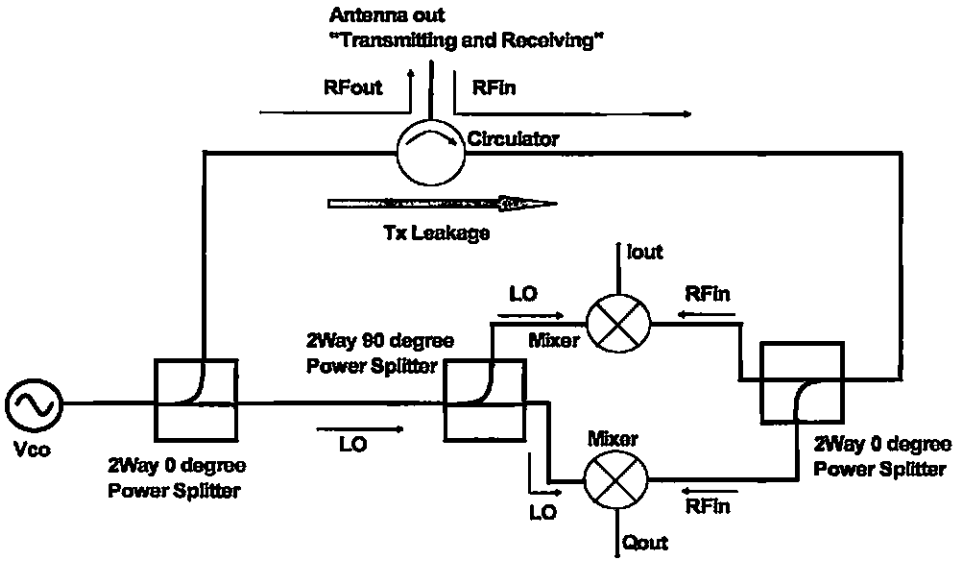

Fig. 5.1. Tx leakage of the transceiver system

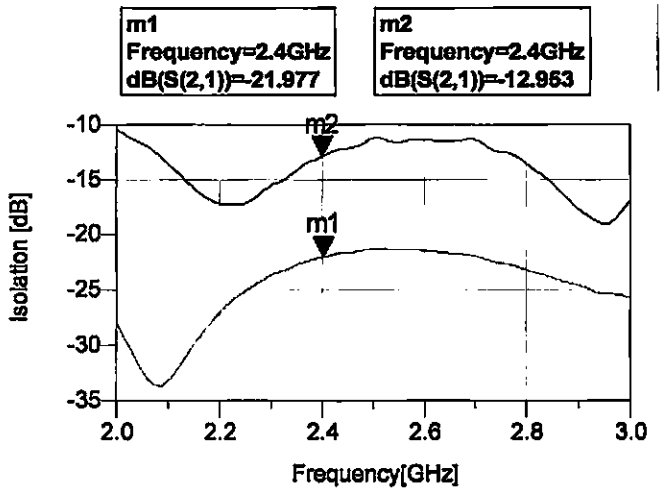

Fig. 5.2. Measured results for isolation of coaxial and surface mount circulator

Because of this isolation, the Tx leakage signal which frequency is same as LO signal inputted to RF port of the mixer, and it makes DC offset and $2f_{LO}$. In Fig. 5.3, the output signal and noise in the passive mixer is shown. Although the $2f_{LO}$ component can be eliminated by low pass filter, due to the DC offset, flicker noise in the output is generated,

and it degrade the sensitivity of the system. If this DC offset can be suppressed, the sensitivity of the system will be improved.

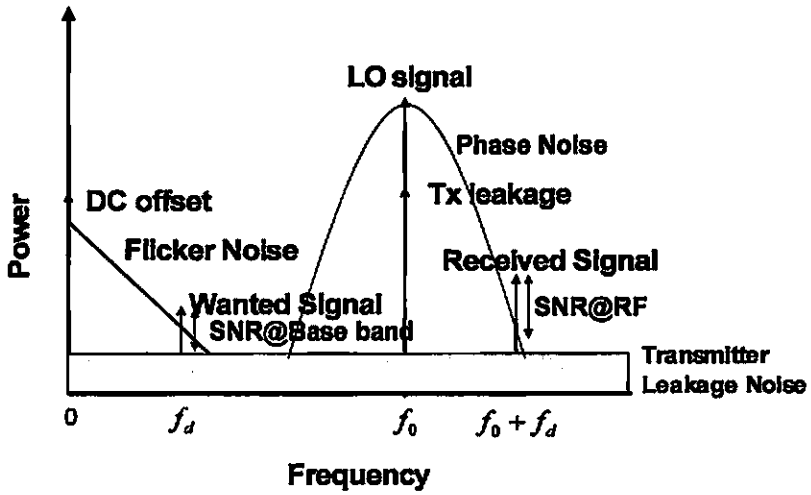

Fig. 5.3. Output signal and noise in a passive mixer

5.1.2 LO Leakage

In the two antenna configulation shown in Fig. 5.4, the LO leakage from the mixer RF port can be serious problem. If there is mismatching in the Rx chain, the leakage signal is reflected and sent to the RF port of the mixer which produces a DC offset. As described above, this DC offset degrades the sensitivity of the system. Also the LO leakage signal can be transmitted by the receiving antenna which affects to the antenna pattern. Therefore to increase sensitivity and to avoid the radiation, an LO leakage cancelion technique is required.

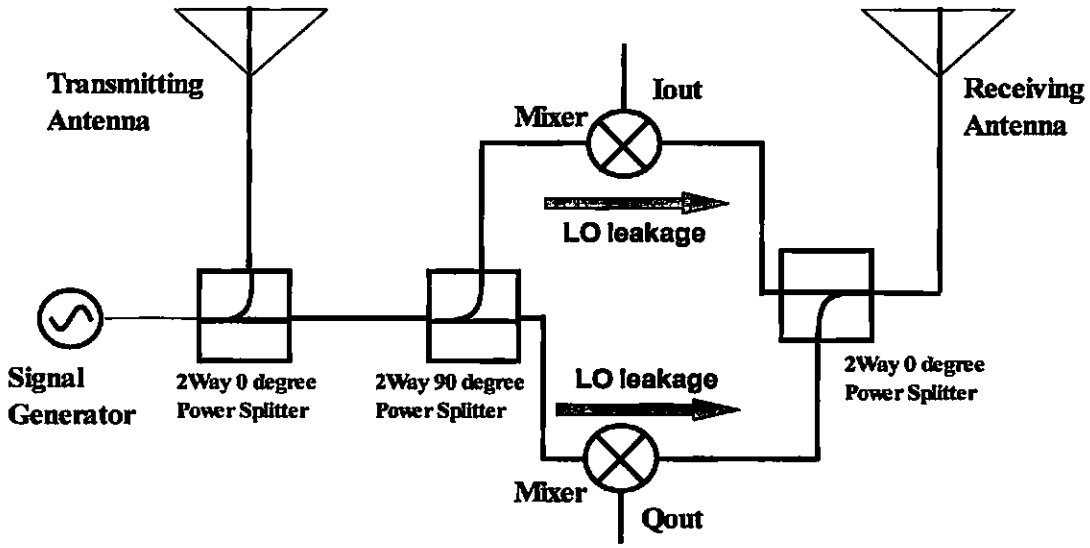

Fig. 5.4. LO signal leakage from the mixer in the multiple antenna configuration

In Fig. 5.5, the LO leakage power measurement setup is shown. In this measurement, coaxial components are used to assemble a quadrature direct conversion system. To the RFin port, spectrum analyzer is connected to measure the LO leakage power. The input signal from the signal generator was 3dBm to deliver 0dBm signal power to the mixer LO port. The measured results are shown in Table 5.1. In this case the LO leakage power was -29.4dBm. Normally that LO leakage signal inputted to receiving antenna and radiated, it can be affected to the transmitting signal and the antenna beam.

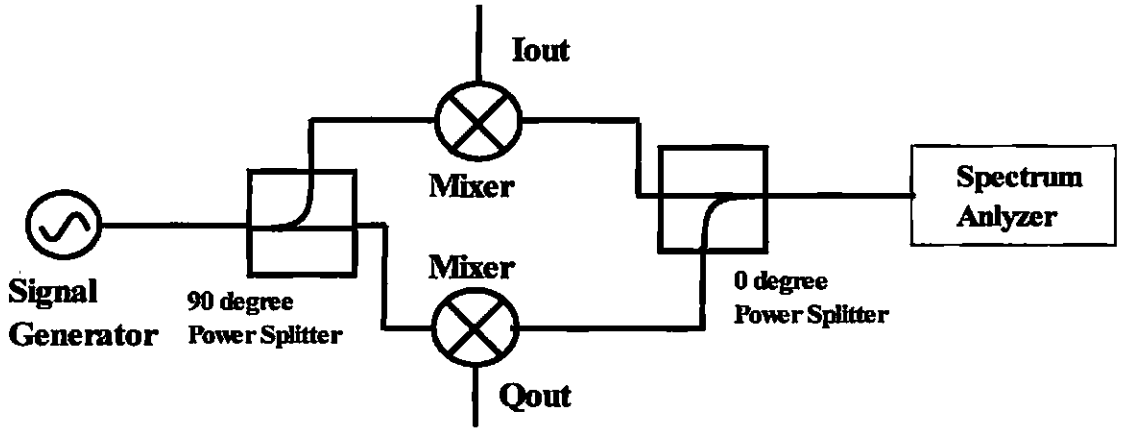

Fig. 5.5. LO leakage power measurement setup

Table 5.1. Measured results for LO leakage power from the mixers

	LO Input	LO leakage
Power[dBm]	0	-29.4

5.1.3 Internal DC Offset of the Mixer

In Fig. 5.6, the measurement setup for the mixer internal DC offset level is shown. In Fig. 5.7, the measured result of DC offset level is shown. From this result, even other DC offset components were eliminated, and there was only 20mV of DC as the main component of DC offset in the system. Even if the system has high Tx to Rx isolation, the Mixer makes DC offset by itself and the DC offset induces the 1/f noise. The flicker noise affects the sensitivity limitation of Doppler radar heart beat detection. Therefore in order to improve the sensitivity, a compensation technique must use to eliminate or reduce this DC offset.

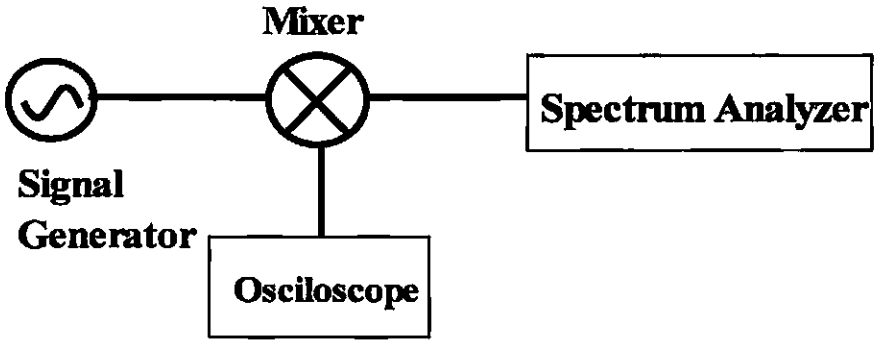

Fig. 5.6. Measurement setup for DC offset of the mixer

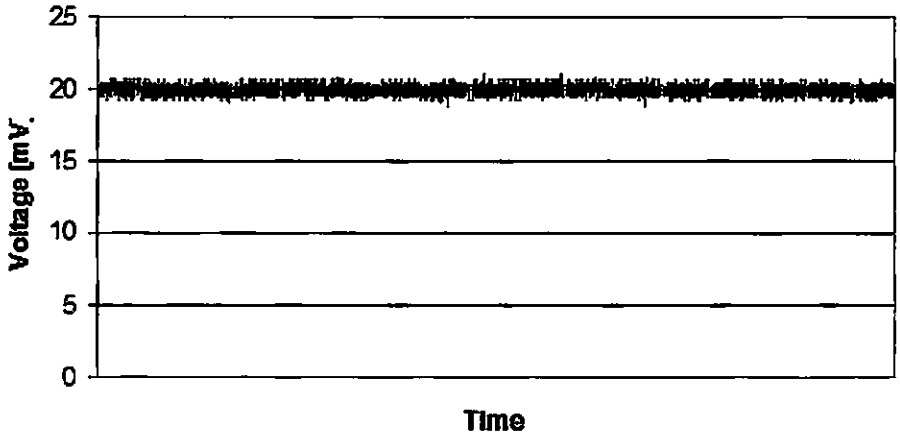

Fig. 5.7. Measured results for DC offset level

5.2 Improvements

5.2.1 Tx Leakage Canceller

In Fig. 5.8, a Tx leakage canceller is shown. This circuit is uses a 180 degree hybrid coupler with three functions[14]: separating Tx and Rx signals, generating the quadrature signal, and improving the Tx to Rx isolation. The signal source is output to LO_I, LO_Q, and the antenna port. The RF port is the isolation port for the Tx signal. On the other hand, the RFin signal received by the antenna is output to the RF port. For the RFin signal, the LO ports are the isolation ports. In Fig. 5.9 and Table 5.2, the simulation schematic for Transmission chain and the simulation results are shown. From this results, the phase difference between I and Qout was 88.716 and Tx to Rx isolation was -39.39dB.

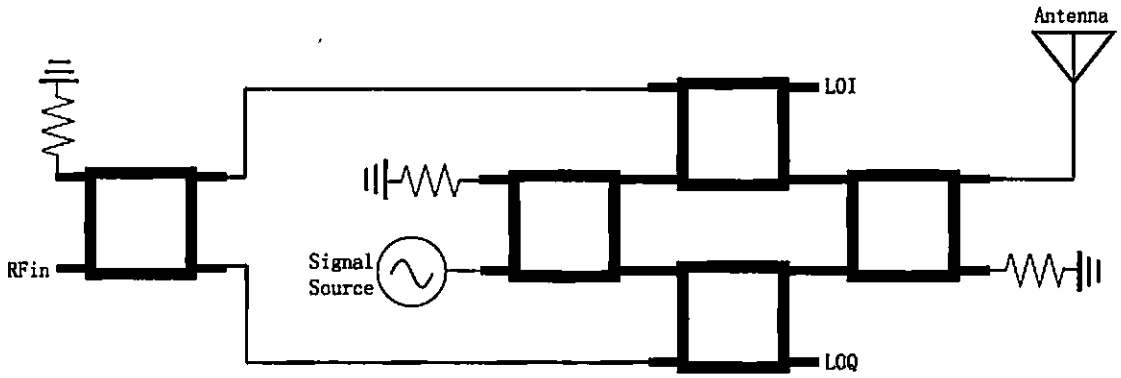

Fig. 5.8 Transmission chain using 90 degree hybrid coupler

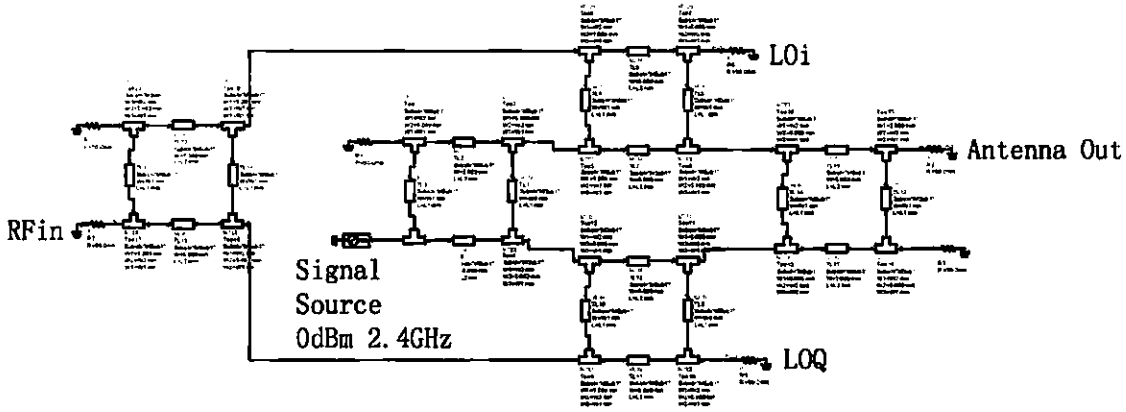

Fig. 5.9. Simulation schematic for transmission chain

Table 5.2 Tx characteristic Simulation results

	Antenna Out	Loi	LOQ	RFin
Power [dBm]	-3.942	-6.626	-6.61	-39.39
Phase [deg]		-11.062	77.654	

In Fig. 5.10, simulation schematic of Rx chain is shown. In this simulation, outputs are RFin, LOi and Q, and signal source ports. The signal is inputted from the antenna port as RFin signal. Although in the actual system, the RFin signal power is very small, less than -20dBm, because the signal was reflected by the object, in this simulation, 0dBm signal power was used to estimate the operation of this circuit. In Table 5.3, the simulation results are shown. The Rx to Tx isolation were -27.906dB of Iout and -26.919dB of Qout. Although there is

inputted RF signal to signal source port, as described above, the RFin signal is small in the actual system. There fore it does not affect too much. To the RFin port, -3.931dBm of RFin signal could be gotten. By comparison to the circulator configuration, there is 3dB loss in Rx chain because of the 90 hybrid, this circuit has good Tx to Rx isolation.

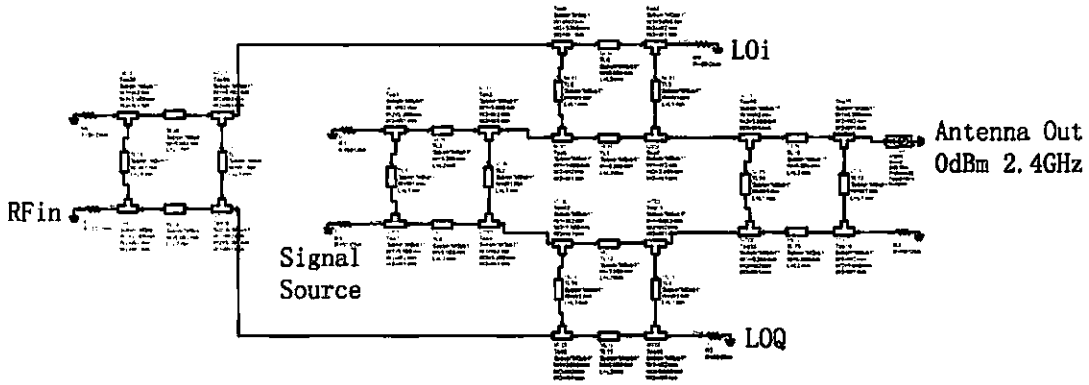

Fig. 5.10. Simulation schematic for receiver chain

Table 5.3. Simulation results

	Signal Source	LOi	LOQ	RFin
Power [dBm]	-3.942	-27.906	-26.919	-3.931

5.2.2 Direct Conversion Circuit with an Isolator

The easiest ways to reduce such LO leakage power is to use an isolator in the Rx chain. As shown Fig. 5.11, an isolator is installed in Rx chain and it imposes directionality on the signal. RFin can pass through the isolator and inputted to the RF port of the mixer. The LO leakage is attenuated by the isolator. In Fig. 5.12, the measurement setup for LO leakage is shown. In this measurement, instead of the isolator, two circulators were used and one port was terminated to realize the isolation. In Table 5.4, the measured results are shown. From this results, the LO leakage was decreased from -29.4dBm to -50dBm.

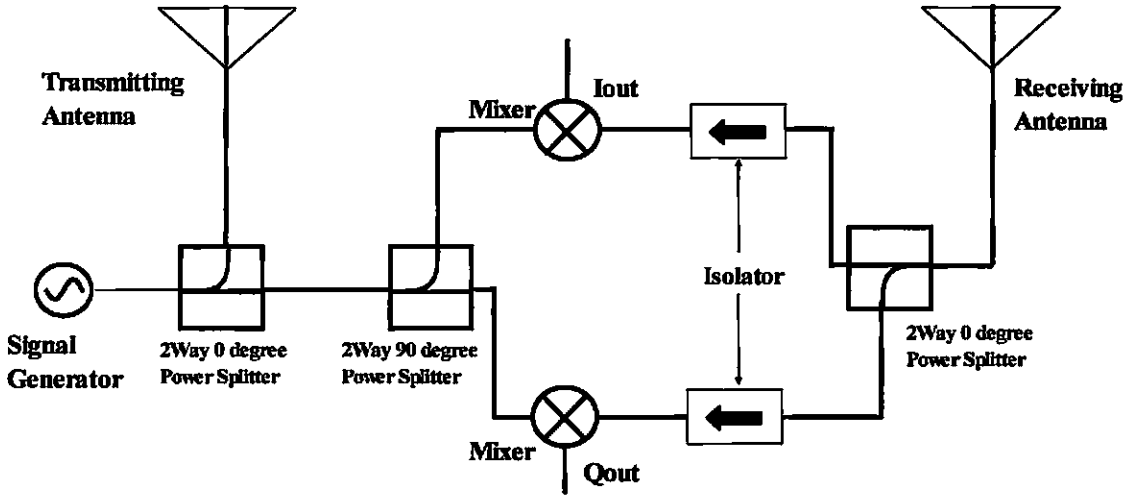

Fig. 5.11. Multiple antenna configuration with Isolator

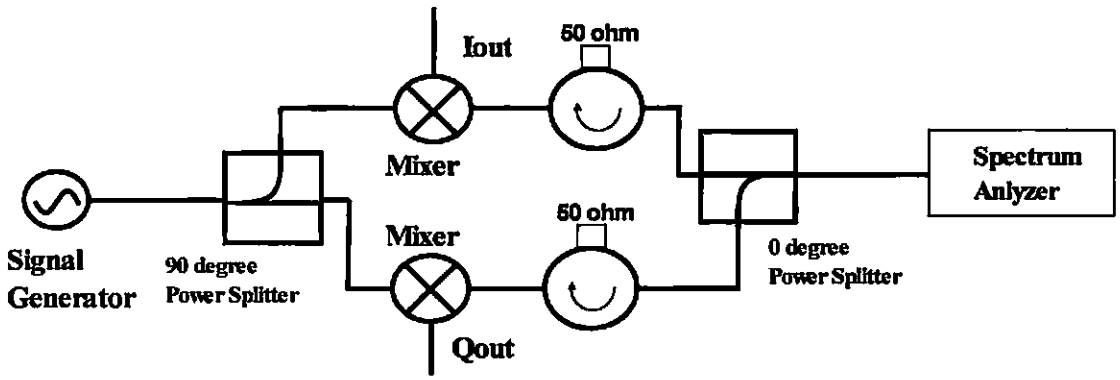

Fig. 5.12. Measurement setup for LO leakage

Table 5.4. Measured results for LO leakage power

	LO Input	LO leakage
Power[dBm]	0	-50

5.2.3 Tx and LO Leakage Canceller

As described above, there is Tx leakage from the circulator in transceiver configuration. However there is also LO signal leakage from poor LO to RF isolation of the mixer. This LO leakage can be used for Tx leakage canceling by adjusting the phase of signal. In Fig. 5.13, the Tx and LO leakage canceller measurement setup is shown. In this

measurement, a phase shifter is installed in Tx chain to change the phase of Tx leakage to make 180degrees phase difference to the LO leakage signal.

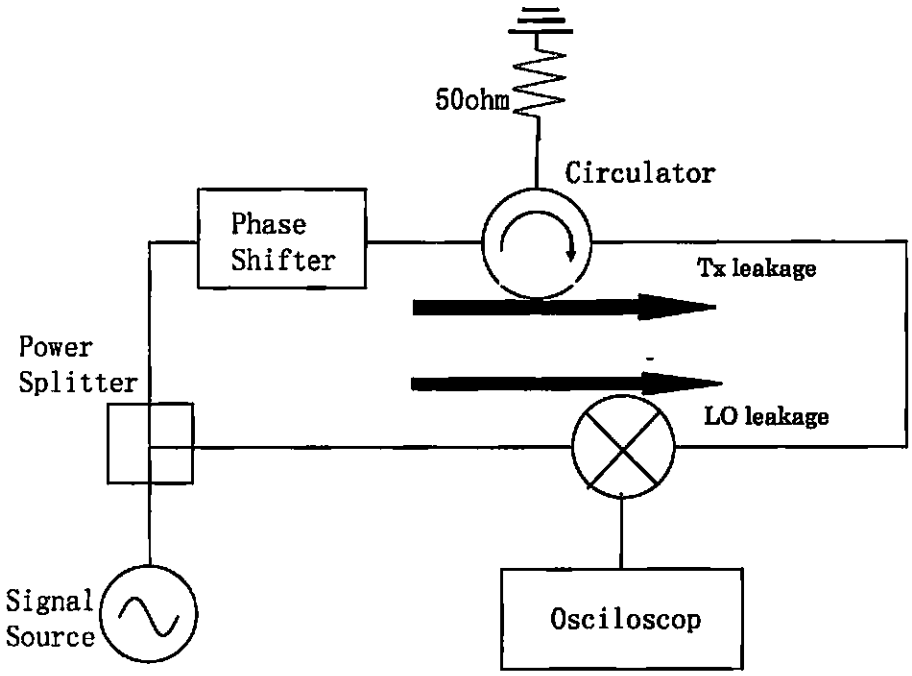

Fig. 5.13. Measurement setup for Tx and LO leakage canceller

In Fig. 5.14, the measured results are shown. There are the maximum and minimum DC offset value due to the phase of Tx leakage signal. The maximum case (i.e. worst case) was 65mV of DC offset, and minimum case (i.e. best case) was 6mV of DC offset were achieved. The LO input power was 7dBm for both case. From this results, just adjusting the phase by adjusting the transmission line, Tx and LO leakage can be cancelled and DC offset can be minimize. In Fig. 5.15, the optimized DC offset of I and Q channel is shown. By the adjusting the phase, 7mV of DC offset for both I and Q channel could be achieved.

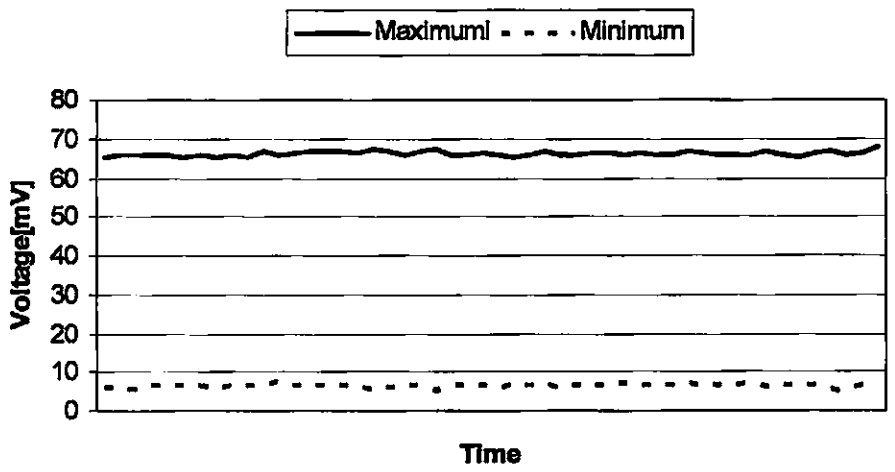

Fig. 5.14. Measured results for DC offset with/without Tx leakage compensation

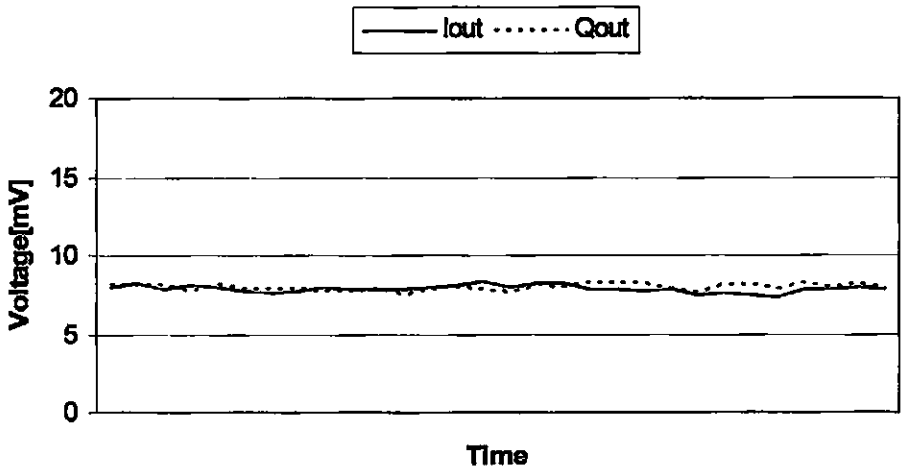

Fig. 5.15. Optimized DC offset of I and Q

In Fig. 5.16, the measured flicker noise of both case are shown. By the phase adjusting technique, 21.7dB of flicker noise power differences between maximum and minimum cases were achieved. From these results, an optimized value of DC offset in transceiver exists and affects to flicker noise.

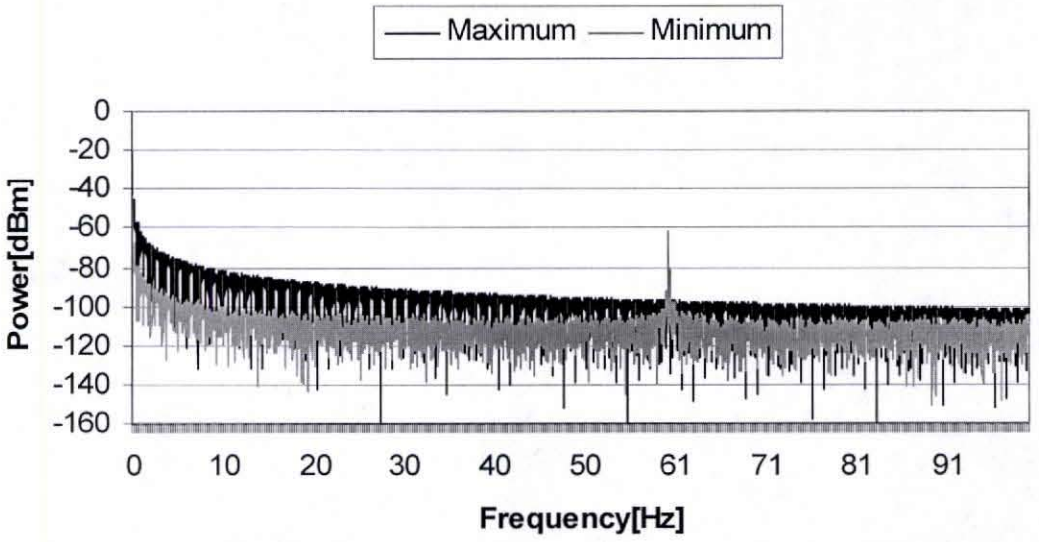

Fig. 5.16. Mesured results of flicker noise power

5.2.4 DC Offset Canceller

In Fig. 5.17, the proposed DC offset compensation block diagram and the measurement setup are shown. By using a power splitter, attenuator, and phase shifter, an LO signal pass through is made to compensate the LO leakage. The phase of the signal is adjusted to a 180 degree phase difference from the LO leakage. The signal is input to the RF port of the mixer through another 0degree power splitter, it compensate the LO leakage. In Fig. 5.18, the measured conversion loss of normal mixer and mixer with bypass is shown. For this configuration, there is only a little a loss from the insertion loss of the 0degree power splitter in receiver chain, and the bypass configuration does not affect the mixer operation.

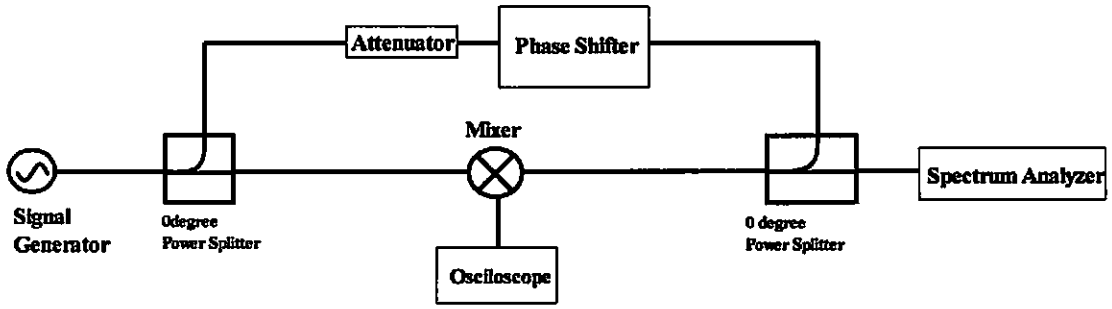

Fig. 5.17. Proposed DC offset canceller block diagram and measurement setup

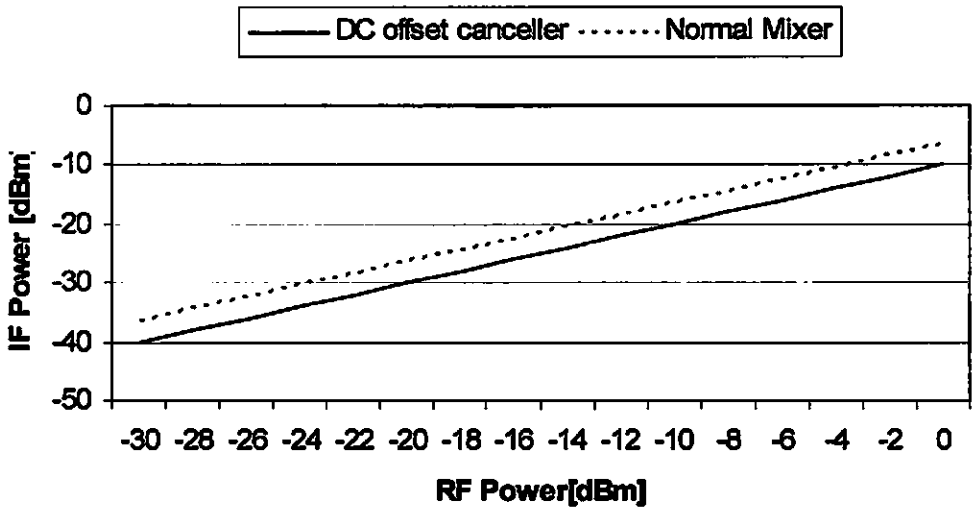

Fig. 5.18. Measured conversion loss for Normal mixer and DC offset canceller

In Fig. 5.19, the measured result of DC offset is shown. In normal case, the DC offset was 20mV. In other hand, with bypass, the DC offset is almost 0mV. Also the LO leakage power was decreased from -19dBm (normal mixer) to -36.72dBm (DC offset canceller). In Fig. 5.20, the measured results of flicker noise in both cases are shown. From this results, 19.3dB of the flicker noise power at 1Hz was achieved by the proposed DC offset canceller.

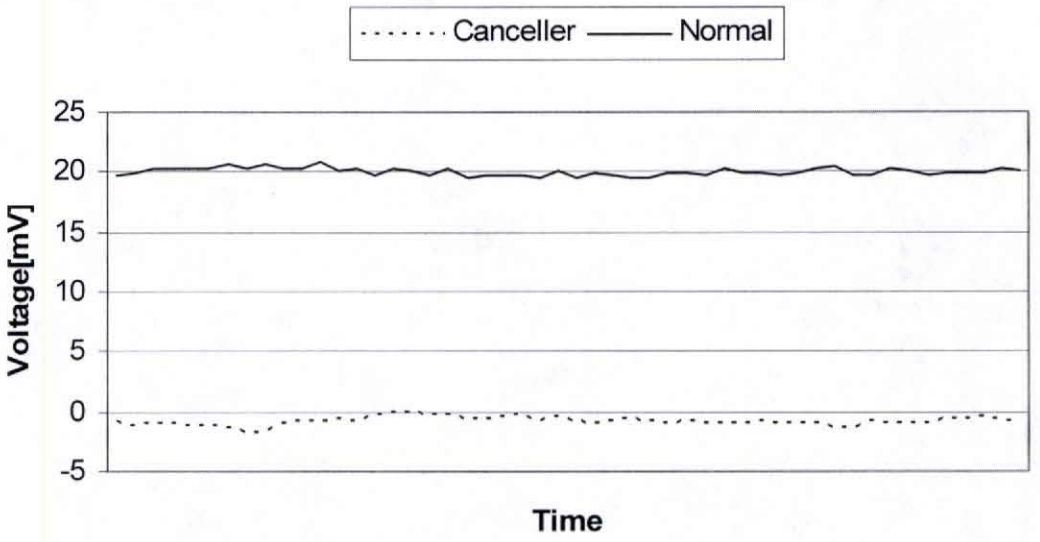

Fig. 5.19. Measured Results of DC offset

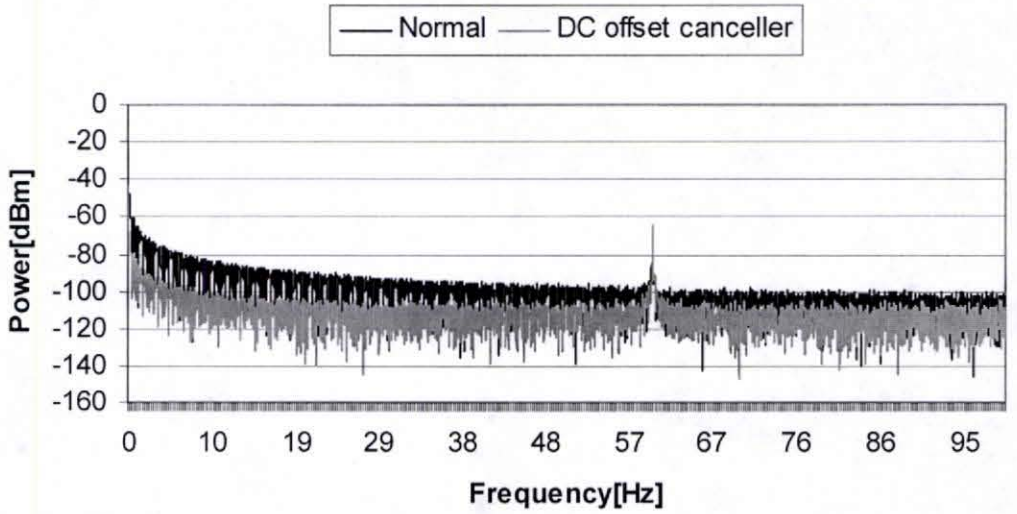

Fig. 5.20. Measured result of flicker noise

CHAPTER6

CONCLUSION

An assessment of requirements and critical specifications for microwave Doppler radar heart rate sensing systems has been presented. In order to realize such a system for effective medical or home use, the first step is to define the specifications which depend on the particular functions and allowable costs. One implementation goal of this research is the fabrication of a handheld heart rate detection system. Obvious system requirements are small size, low cost, ease of use, and safety. However, the most important thing to be considered for a useful heart rate detection system is accuracy and functional limitations, which present certain trade-offs with other requirements. Assessing the minimal needs and maximum tolerance for each or these items is essential for an effective system design.

The limitations and requirements for the system were assessed in Chapter 3. The fundamental limitations for transmit and receive power versus range for a functional 2.4GHz IMS band cardiopulmonary radar system were computed and measured, including free space losses, and fundamental heart rate detection limits. The minimum required power for close range rate detection was also assessed. At a 1m distance between the transmitting antenna and target, which is presupposed as a standard distance for heart rate detection, the free space loss was determined to be 40dB, which defines the fundamental detection limit. For measurement of round trip power of the signal which is reflected by the target, the direct coupling problem between transmitter and receiver which causes overestimation of the signal power must be considered. In order to accurately measure the round trip signal power, a

direct coupling canceling technique was proposed and used for the measurement. By using the technique, the direct coupling signal was cancelled and -37dBm of signal power was achieved at 1m distance with 0dBm of transmitted power from the antenna. Based on calculations and measurements, the minimum limit for transmitted power was also assessed. Heart rates for subjects holding their breath and subjects breathing normally were successfully tracked for signal power levels as low as 20 nW. This is the lowest power ever reported for ISM band CW Doppler radar heart rate detection. These results can be extrapolated to larger power systems where obstructions and antenna gain similarly impact the signal power available for heart motion detection.

Based on the assessment of the system functions and consideration of the requirements, a 2.4GHz microwave Doppler radar system was designed and fully integrated on a printed circuit board. The design and measured results for the fabricated PCB were described in Chapter 4. The transceiver and multiple antenna configurations were composed and fabricated based on different requirements and considerations. This system was separated into two parts. One was the LO feed circuit for distributing the LO signal to the transceiver chain and receiver chain. The other was the quadrature direct conversion circuit. Based on this design, the system could be easily expanded as modular system.

In Chapter 5, issues and means for performance improvement for the system were described based on analysis of the measured circuits. Direct conversion circuit has several issues due to components and architecture. In a transceiver configuration, the isolation between Tx and Rx depends on the configuration or components which separate Tx and Rx. Leakage of the TX signal reaches the RF port of the mixer causing self mixing of the LO. This produces a DC offset and induces flicker noise. Flicker noise significantly affects to the

SNR at baseband and degrades the system sensitivity. Also DC offset is induced by LO leakage to the RF port of the mixer. Inadequate LO-RF isolation also causes LO leakage throughout the receiver chain. It can be transmitted by the receiving antenna and may affect both the transmitting antenna and other receiving antenna performance. In order to avoid such problems and improve sensitivity, several circuit configurations were proposed. From the measured results, there are optimum and worst cases for leakage due to the phase relationship between the Tx and LO leakage signals. By adjusting the phase of either signal, the DC offset problem caused by the self mixing signal could be cancelled. For the LO self mixing and leakage problem in the mixer, a novel DC offset and LO leakage canceling configuration was proposed and described. By using these techniques, zero DC offset and 17dB of LO leakage reduction could be achieved. The DC offset canceling technique resulted in a 19.3dB reduction in flicker noise.

These results indicate that effective heart rate sensing can be developed with practical microwave hardware, provided that appropriate measures are applied to mitigate the issues described here.

REFERENCES

[1] V.M. Lubecke, O. Boric-Lubecke, G. Awater, P.-W. Ong, P. Gammel, R.-H. Yan, J.C. Lin, "Remote Sensing of Vital Signs with Telecommunications Signals," (Invited) presented at the World Congress on Medical Physics and Biomedical Engineering (WC2000), Chicago, IL, USA, July 2000.

[2] A. Droitcour, V. M. Lubecke, J. Lin, and O. Boric-Lubecke, "A Microwave Radio for Doppler Radar Sensing of Vital Signs," IEEE MTT-S International Microwave Symposium, Phoenix, AZ, USA, vol. 1, pp. 175–178, May 2001.

[3] A. D. Dritcour, O. Boric-Lubecke, V. M. Lubecke, J. Lin and G. T. Kovacs, "Range Correlation and I/Q Performance Benefits in Single Chip Silicon Doppler Radars for Non-Contact Cardiopulmonary Monitoring" IEEE Trans. on Microwave Theory and Tech., Vol. 52, No. 3, pp. 838-848, March 2004.

[4] Y. Xiao, J. Lin, O. Boric-Lubecke, V. Lubecke, "Frequency tuning technique for remote detection of heartbeat and respiration using low-power double- sideband transmission in Ka-band" IEEE Transactions on Microwave Theory and Techniques, Vol. 54, No. 5, pp. 2023-2032, May 2006.

[5] Byung-Kwon Park, Shuhei Yamada, Olga Boric-Lubecke, and Victor Lubecke, "Single-Channel Receiver Limitations in Doppler Radar Measurements of Periodic Motion," IEEE Radio and Wireless Symposium, San-diego, CA, January 2006.

[6] A. D. Droitcour, O. Boric-Lubecke, V. Lubecke, J. Lin, and G. T. A. Kovacs, "0.25 um CMOS and BiCMOS single-chip direct-conversion Doppler radars for remote sensing of vital signs," in Int. Solid-State Circuits Conf. Dig., vol. 1, San Francisco, CA, 2002, p. 348.

[7] A. A. Abidi, "Direct-conversion radio transceiver for digital communications," *IEEE J. Solid-State Circuits,* vol. 30, no. 12, pp. 1399-1410, Dec. 1995.

[8] A. D. Droitcour, O. Boric-Lubecke, V. M. Lubecke, J. Lin and G. T. Kovacs, "Range correlation and I/Q performance benefits in singlechip silicon Doppler radars for non-contact cardiopulmonary
monitoring," *IEEE Trans. Microwave Theory Tech.*, vol. 52, no. 3, pp. 838-848, March 2004.

[9] A. Loke and F. Ali, "Direct conversion radio for digital mobile phones design issues, status, and trends," *IEEE Trans. Microwave Theory Tech.,* vol. 50, no 11, pp. 2422-2435, Nov. 2002.

[10] R. Moraes and D.H. Evans , "Compensation for phase and amplitude imbalance in quadrature Doppler signals," *Ultrasound Med. Biol.,* vol.22, pp. 129-137, 1996.

[11] F. E. Churchill, G. W. Ogar and B. J. Thompson, "The correction of I and Q errors in a coherent processor," *IEEE Trans. Aerospace and Electronic Systems*, vol. AES-17, no. 1, pp. 131-137, Jan. 1981.

[12] Z. Zhu and X. Huang, "Gain/phase imbalance and DC offset compensation in quadrature modulators," *IEEE International Circuits and Systems Symposium,* 2002, vol. 4, pp. 811-814.

[13] H.-H. Chen, J.-T. Chen and P-C. Huang, "Adaptive I/Q imbalance compensation for RF transceivers," *IEEE Global Telecommunications Conference*, 2004, vol. 2, pp. 818-822.

[14] Choul-Young Kim, Jeoung-Geun Kim, and Songcheol Hong, "A Quadrature Radar Topology with Tx Leakage Canceller for 24GHz Radar Applications"

[15] Amy Droitcour, Olga Bolic-Lubecke, Victor M. Lubecke, Jenshan Lin, and George T.A. Kovacs, "Chest Motion Sensing with Modified Silicon Base Station Chips," IEICE Trans.Electron., Vol.E87-C, No9 September 2004.

[16] Amy Droitcour, Olga Bolic-Lubecke, Victor M. Lubecke, Jenshan Lin, and George T.A. Kovacs, "Quadrature Phase Demodulation in detection of Heart Rate with a Single Chip Doppler Radar Transceiver"

[17] Mervin C. Budge Jr, and Mickie P. Burt, "Range Correlation Effects in Radars," IEEE Radar Conference 1993

[18] Mickie P. Burt and Mervin C. Budge Jr, "Range Correlation Effects on Phase Noise Spectra," IEEE System Theory, 1993.